# Beam Manipulation Using Lasers

- Laser Slicing
- Laser Heating
- Optical Stochastic Cooling
- FEL seeding with High Harmonics
- ESASE
- EEHG (Echo FEL)

# Laser Slicing

## Why Slice?

- Useful to have a bright x-ray probe at the 100 fsec level
  - eg in condensed matter, probes on phonon time scales
  - Not so bright options
    - laser plasma source
    - Thomson scattering
    - fast detection (eg synch source + streak camera)
- Has become standard to make a user facility with femtoslicing: BESSYII, SLS, ALS, SOLEIL, TPS…

# Laser Slicing Principle

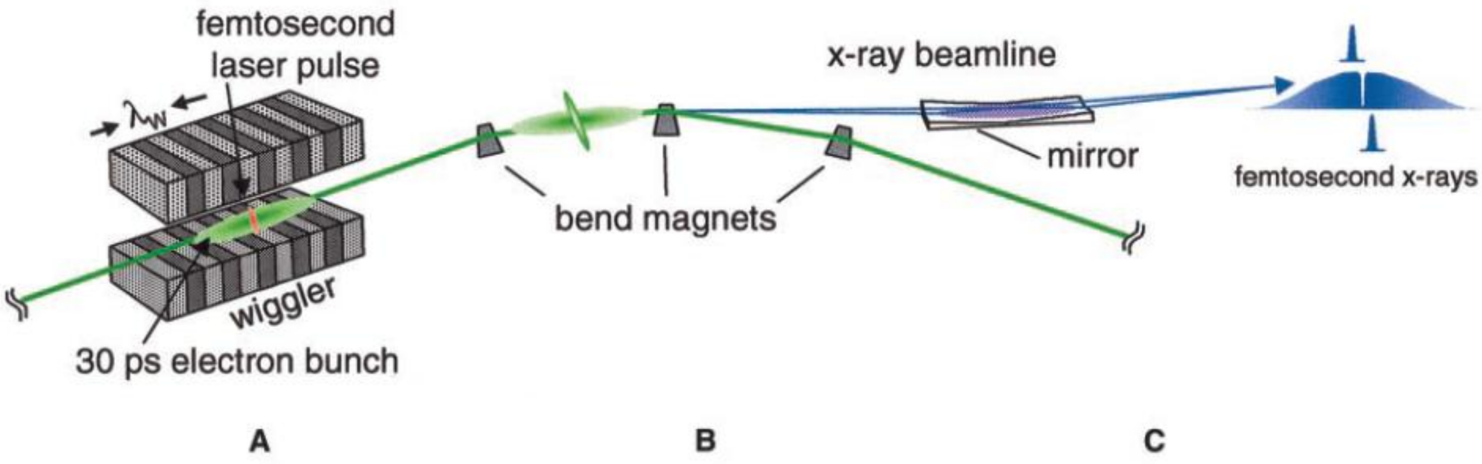


A Overlapping short laser beam with bunch center, meeting the resonance condition,

$$\lambda_L = \lambda_S = \frac{\lambda_W}{2\gamma^2}\left(1+\frac{K^2}{2}\right), \text{where } K = \frac{eB_0\lambda_W}{2\pi mc}$$

modulates the energy in the short "slice"

B In a dispersive bend the modulated beam is separated transversely from the rest of the bunch

C Imaged short pulse radiation is spatially separate from radiation from the "core" (rest of the bunch)

Schoenlein et al Science 287, 2237 (2000)

# Proof of Principle experiment at ALS (2000)

**Fig. 3.** Model calculation of the electron bunch distribution (as a function of horizontal displacement Δx and time) at the radiating bend magnet, following interaction with the laser pulse in the wiggler, and propagation through 1.5 arc sectors of the storage ring.

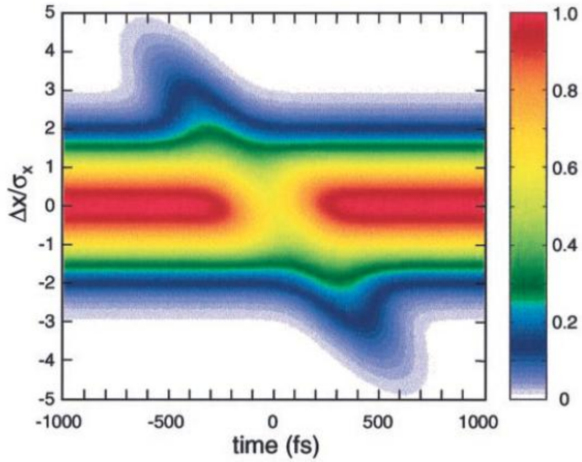


spatially-resolved cross-correlations of visible synchrotron radiation

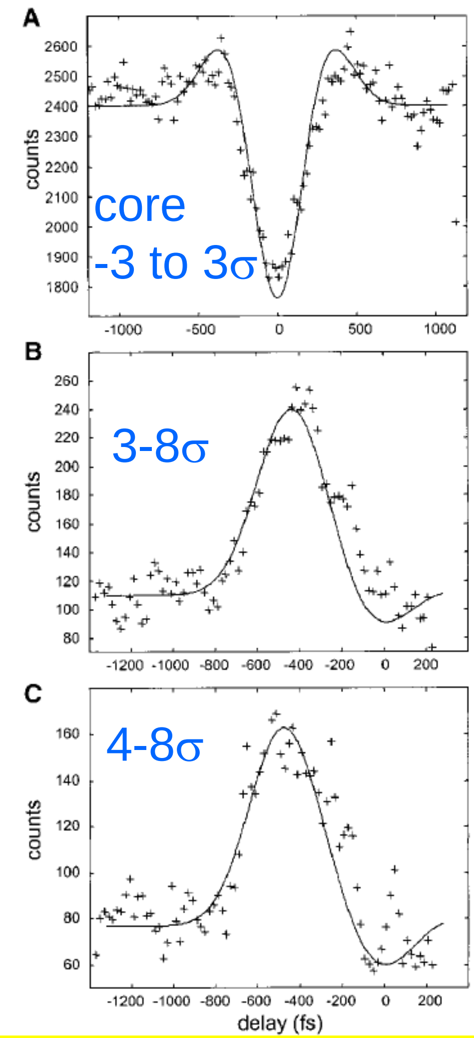


Predicted & observed Gain in Laser Pulse

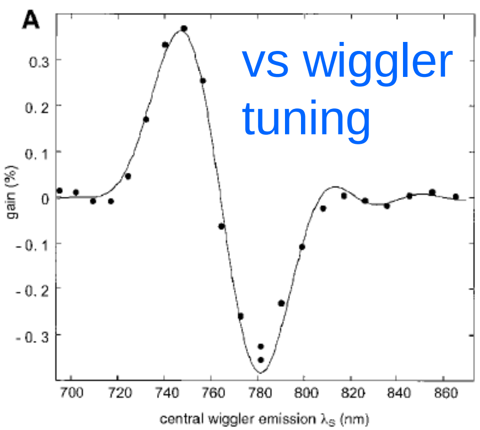


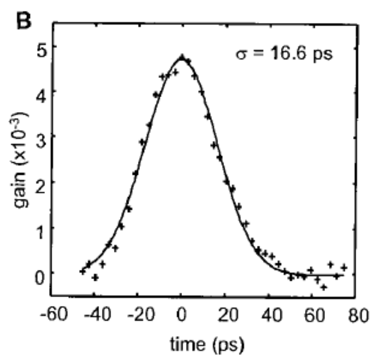


vs position in bunch

E=1.5 GeV, $\sigma_E$=1.2 MeV,

Udulator: $L_U$=3 m, K=13, $\lambda_U$=16 cm

Laser: λ=800 nm, $\tau_L$=100 fs, power W=4 GW (0.4 mJ per pulse), 1 kHz

Schoenlein et al Science 287, 2237 (2000)

# Laser Slicing

Gets tougher as you go to higher energy rings

- Requires energy modulation $\Delta E$ a few times greater than beam energy spread $\sigma_E$
  - required laser energy scales as $\Delta E^2$
- need to do in near-IR, where energetic short pulse lasers are available, but wiggler period scales as $\gamma^2$
- For APS @ 7GeV, this would mean 12 mJ laser, $\lambda_W$=65 m

Typical fluxes $10^4$-$10^5$ photons/sec/0.1%BW

- TPS projects as high as $10^7$

Contributions to pulse width

- laser pulse width
- slippage in undulator
- emittance
- energy dispersion

Projections for SOLEIL slicing source

Table 2: Duration of the Pulse (FWHM in fs).

| Radiator | Laser | Slippage | Emittance | Energy | Total |
|---|---|---|---|---|---|
| CRISTAL | 50 | 53 | 54 | 52 | 104 |
| TEMPO | 50 | 53 | 47 | 117 | 145 |

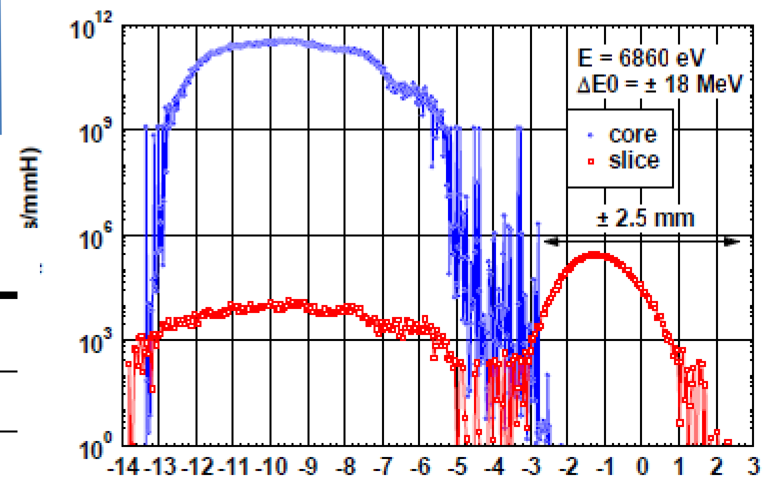


Nadji et al IPAC 10 WEPEA012

# Laser Heating

- LCLS requires strong bunch compression, from ~5 psec to ~200 fsec
- strong compression susceptible to microbunching instability
    - small energy modulations, arising from drive laser, longitudinal space charge, coherent synchrotron radiation, geometric wake fields…
    - in a bend these are converted to small density modulations
    - strong gain for these modulations in the bunch compressor
- introducing a small uncorrelated energy spread along the whole bunch suppresses this effect
    - use IFEL effect using an undulator at low beam energy (135 MeV) & near-IR laser (leftover unconverted drive laser)

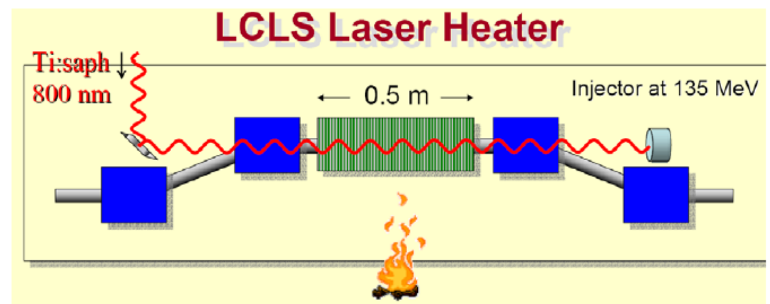


Huang, FEL 04

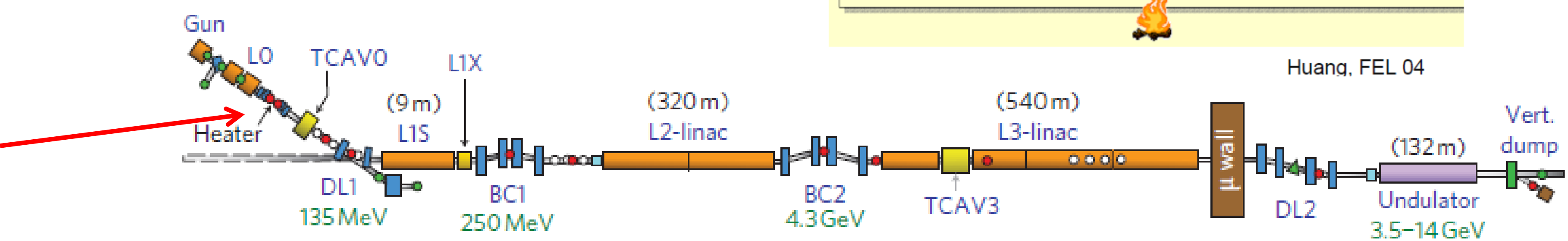


P. Emma et al Nat Phot 4, 641 (2010)

# Laser Heater

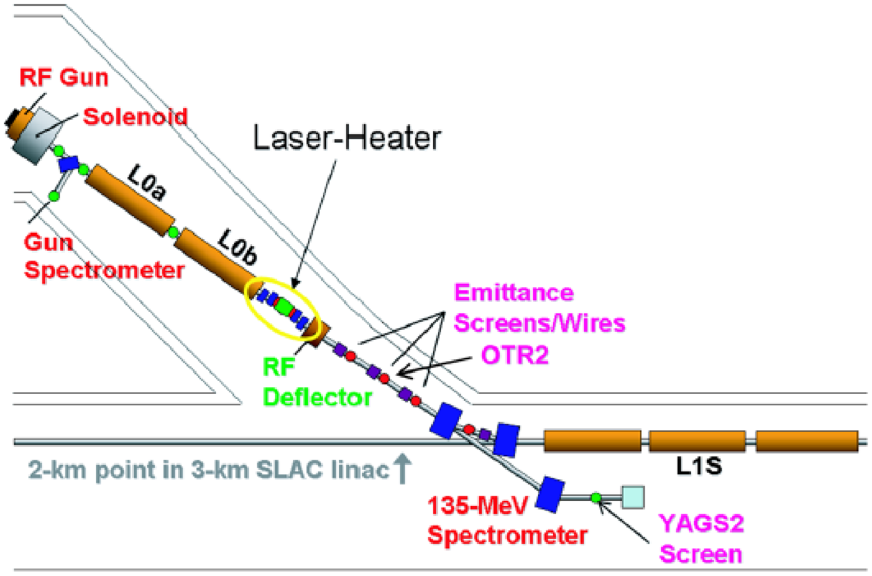


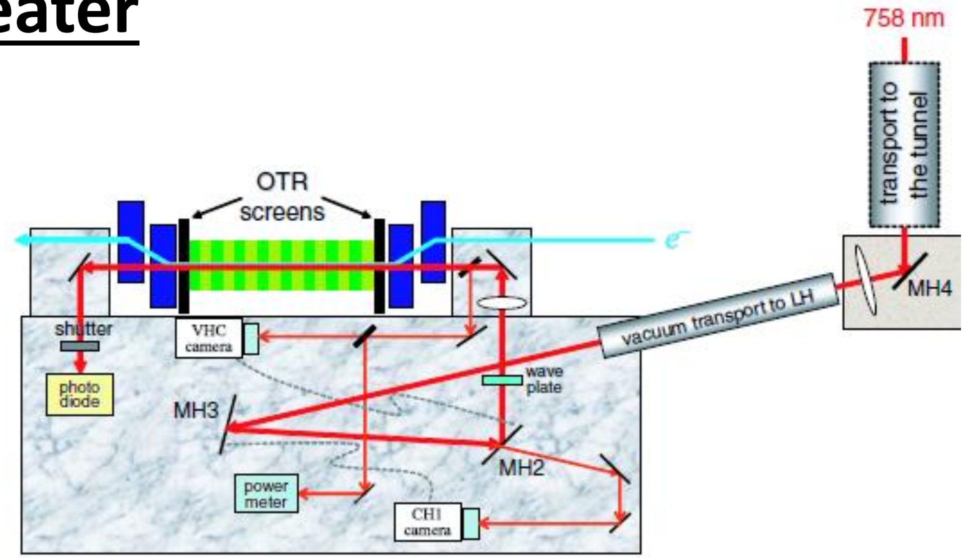


TABLE I. Main parameters for the LCLS laser heater (LH) (at 135 MeV).

| Parameter | Symbol | Value | Unit |
|---|---|---|---|
| LH-undulator pole full gap | $g_u$ | 34.5 | mm |
| LH-undulator parameter | $K$ | 1.38 | |
| LH-undulator period | $\lambda_u$ | 5.4 | cm |
| Number of undulator periods | $N_u$ | 10 | |
| IR-laser wavelength | $\lambda_L$ | 758 | nm |
| IR-laser energy (nominal 6 $\mu$J) | $E_L$ | <230 | $\mu$J |
| IR-laser pulse duration (FWHM) | $T_L$ | 10–20 | ps |
| Horizontal offset at chicane center | $\Delta x$ | 35 | mm |
| Bend angle of each dipole | $\vert\theta\vert$ | 7.5 | deg |
| Chicane momentum compaction | $R_{56}^T$ | 7.8 | mm |
| Electron rms transverse size | $\sigma_{x,y}$ | ~150 | $\mu$m |
| IR-laser rms spot size | $\sigma_r$ | ~210 | $\mu$m |
| Laser Rayleigh length | $Z_R$ | ~70 | cm |

Z Huang et al PRSTAB 13, 020703 (2010)

- Align and match e-beam and laser beam using OTR screens
- Measure energy spread with 135 MeV spectrometer (few keV resolution)

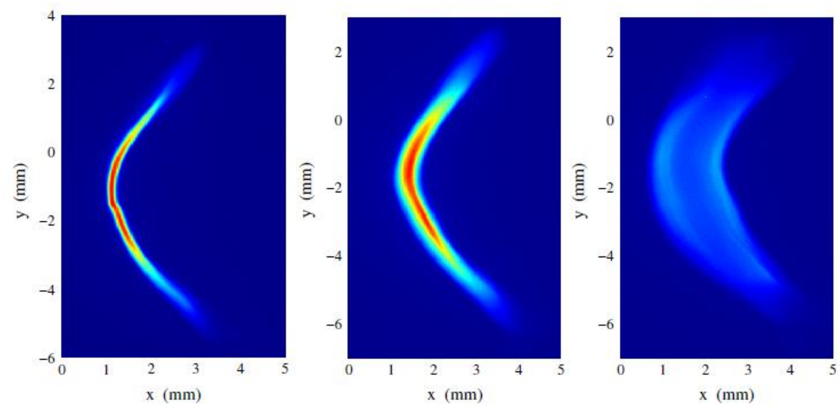


(a) no heating (b) nominal heating (c) maximum heating

# Laser Heater

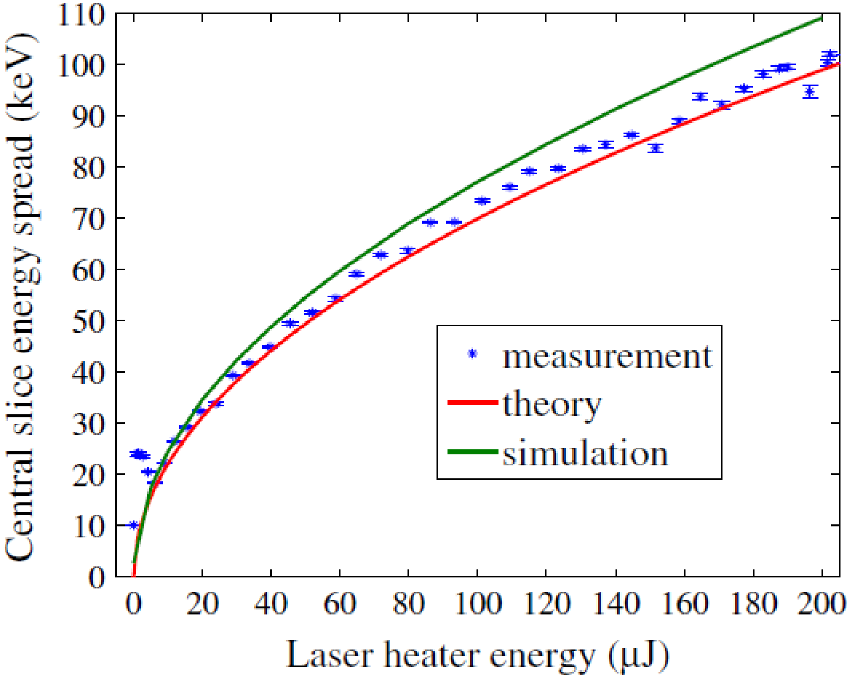


FIG. 8. (Color) Central slice rms energy spread vs LH energy.

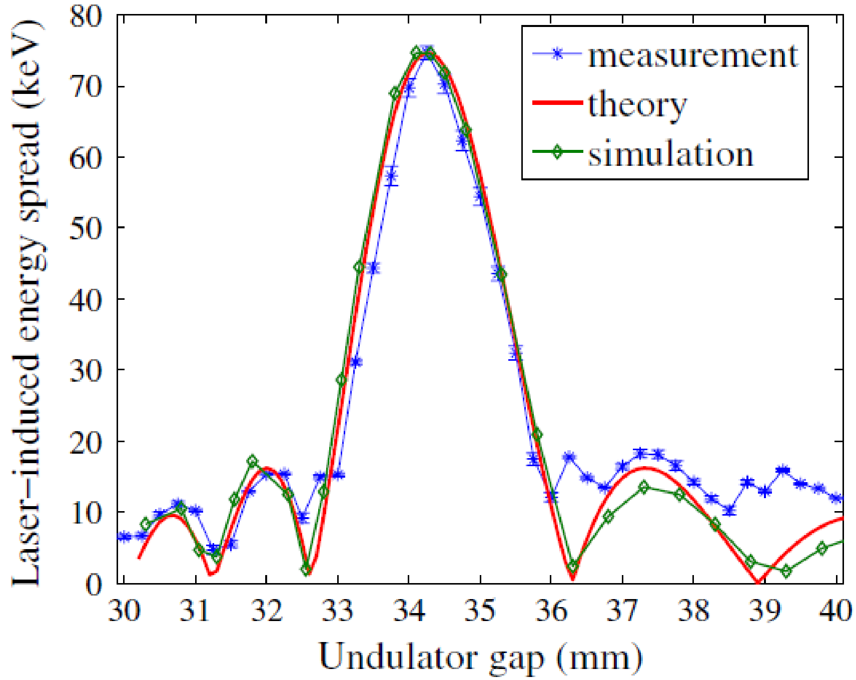


FIG. 9. (Color) Laser-induced rms slice energy spread vs LH-undulator gap (LH energy is about 200 $\mu$J).

LH=laser heater

Z Huang et al PRSTAB 13, 020703 (2010)

# Laser Heating

FEL output energy (unsaturated 12 undulator sections)

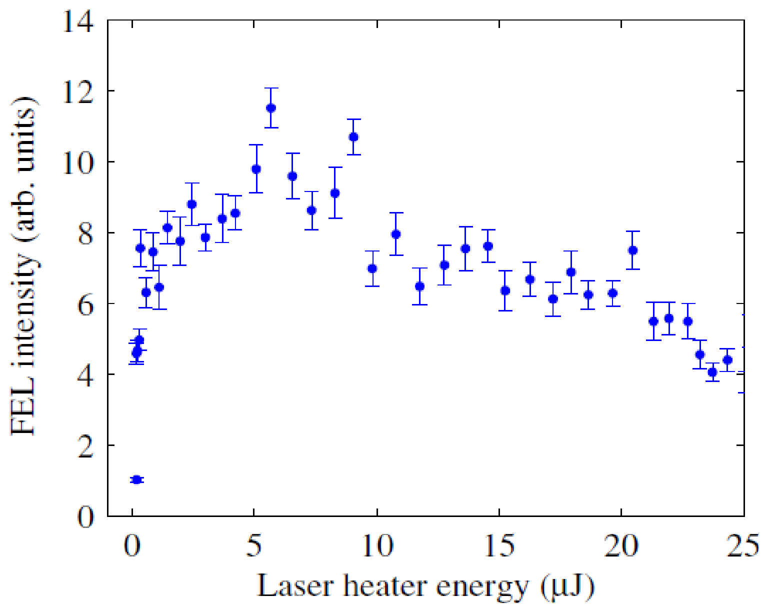


FIG. 15. (Color) FEL intensity at 1.5 Å measured on a downstream YAG screen vs LH energy when 12 undulator sections are inserted.

FEL gain length

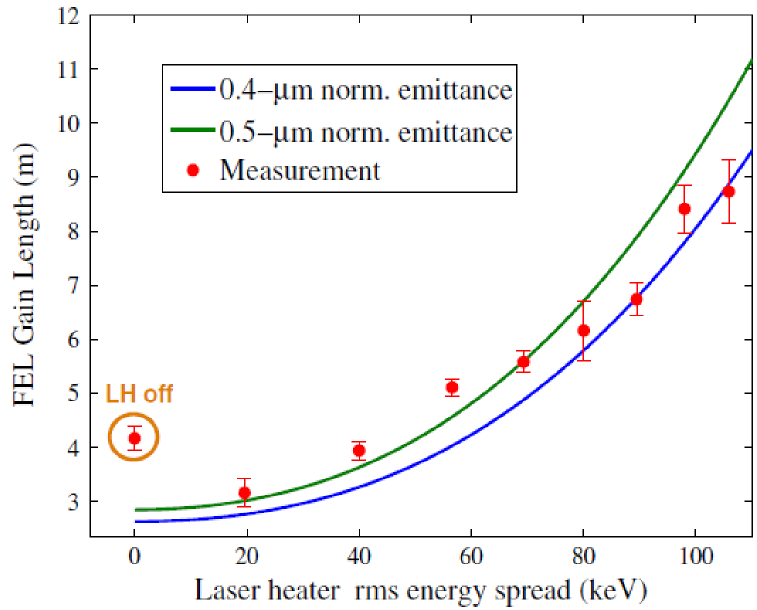


FIG. 16. (Color) FEL gain length at 1.5 Å vs LH-induced energy spread.

- FEL output optimized for very modest heating (6 uJ, 20 keV)
- Gain length vs energy spread consistent with theory
  - high ΔE=0 value (Laser Heater off) due to energy spread arising from microbunching instability

# Optical Stochastic Cooling

- Basic concepts of Stochastic Cooling
- Harmonic Oscillator model
  - cooling/heating
  - bandwidth
- Optical Stochastic Cooling
  - principles
  - issues
  - proposals
- Coherent Electron Cooling

# Stochastic Cooling

Basic Concepts

• detect a particle's motion with a pickup, and correct it downstream with a kicker

• works on the incoherent motion of individual particles, not the coherent motion of the beam as a whole

• But the detector can't resolve individual particles

• a particle sees the sum of its own damping signal and that of other particles

• because particles' frequencies differ slightly, the force from other particles occur at random phase and average to zero in first order

  • can already see that bandwidth is important

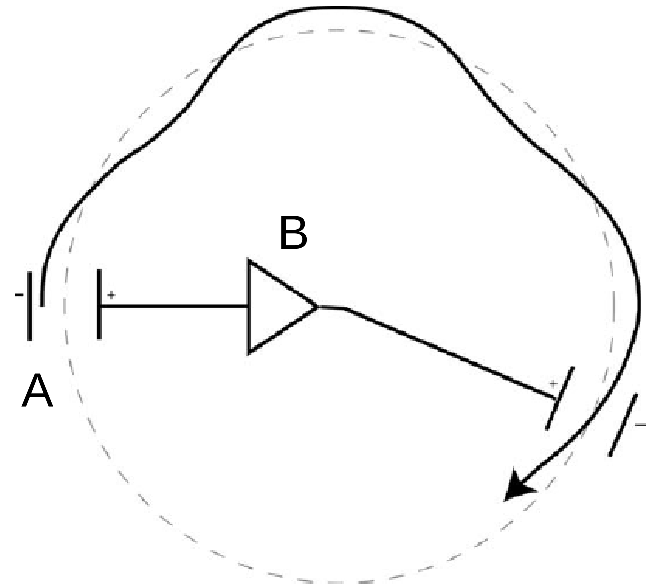


Betatron Cooling

• pickup at A detects position
• signal amplified at B
• momentum correction applied at point C, where betatron phase is 90° relative to A

J. Marriner Nuclear Instruments and Methods in Physics Research A 532, 11 (2004)

# Stochastic Cooling

A Bit of History:

1968: First stochastic cooling theory developed by Simon van der Meer
1975: First test, at Intersecting Storage Rings at CERN
1984: Nobel Prize awarded to van der Meer
- shared with Carlo Rubbia for discovery of W & Z
- stochastic cooling critical for W/Z discovery

1993: Optical Stochastic Cooling Mikhailichenko/Zolotorev
1994: Transit time Optical Stochastic Cooling

Table 1. A list of stochastic cooling systems and basic parameters.

| Site | Machine | Type | Frequency (MHz) | Beam Momentum (GeV/c) |
|---|---|---|---|---|
| CERN | ISR | H & V | 1000-2000 | 26.6 |
| | ICE | H, V, ΔP | 50-375 | 1.7 & 2.1 |
| | AA | PreCool ΔP<br>ST H, V, ΔP<br>Core H, V, ΔP | 150-2000 | 3.5 |
| | LEAR | 2 systems<br>H, V, ΔP | 5-1000 | <0.2 &<br>0.2-2.0 |
| | AC | H, V, ΔP | 1000-3000 | 3.5 |
| | AD | H,V, ΔP | 900-1650 | 2.0 & 3.5 |
| FNAL | ECR | V, ΔP | 20-400 | 0.2 |
| | Debuncher | H, V, ΔP | 4000-8000 | 8.9 |
| | Accumulator | ST ΔP<br>Core H, V, ΔP | 1000-8000 | 8.9 |
| KFA Julich | COSY | H, V, ΔP | 1000-3000 | 1.5-3.4 |
| GSI Darmstadt | ESR | H, V, ΔP | 900-1700 | 0.48/nucleon |
| Tokyo | TARN | ΔP | 20-100 | 0.007 |
| BINP | NAP-M | ΔP | 100-300 | 0.062 |



J. Marriner Nuclear Instruments and Methods in Physics Research A 532, 11 (2004)

# Stochastic Cooling

- Think N particles as a set of harmonic oscillators

$$x_i(t) = A_i \cos(\omega_i t + \phi_i), \quad i = 1,2,\dots,N$$

- At certain time *t*, the average position

$$\bar{x}(t) = \frac{1}{N}\sum_{i=1}^{N} x_i(t), \quad \overline{x^2}(t) = \frac{1}{N}\sum_{i=1}^{N} x_i^2(t)$$

- And the time average

$$\left\langle \bar{x}(t) \right\rangle = \lim_{T\to\infty} \frac{1}{2T}\int_{-T}^{T} \frac{1}{N}\sum_{i=1}^{N} x_i(t)dt = 0$$

$$\left\langle \overline{x^2}(t) \right\rangle = \lim_{T\to\infty} \frac{1}{2T}\int_{-T}^{T} \frac{1}{N}\sum_{i=1}^{N} x_i^2(t)dt = \frac{1}{2N}\sum_{i=1}^{N} A_i^2$$

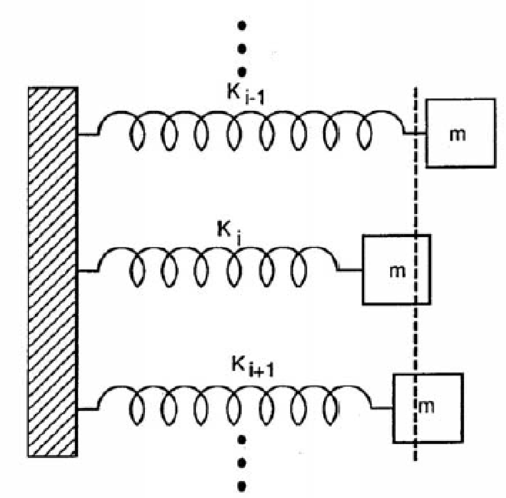


$$\lim_{T\to\infty} \frac{1}{2T}\int_{-T}^{T} \cos(\omega t + \phi)dt = \begin{cases} \cos\phi, \omega = 0 \\ 0, \omega \neq 0 \end{cases}$$

$$\int_{0}^{2\pi} \cos^2(\omega t + \phi)dt = \pi$$

J. Marriner and D. McGinnis, AIP 249, 693 (1992)

# Stochastic Cooling

- Suppose at some time when $\bar{x}(t) \neq 0$, a kick of $\Delta x(t) = -g\bar{x}(t)$ is applied, without changing the speed of the oscillators. The new position is

$$x_{ic}(t) = x_i(t) - \frac{g}{N} x_i(t) - g\frac{1}{N}\sum_{k \neq i}^{N} x_k(t)$$

- So the amplitude of each oscillator becomes a function of time and the rms amplitude is

$$\sigma^2(t) = \left\langle \overline{x^2}(t) \right\rangle = \frac{1}{2N}\sum_{i=1}^{N} A_i^2(t)$$

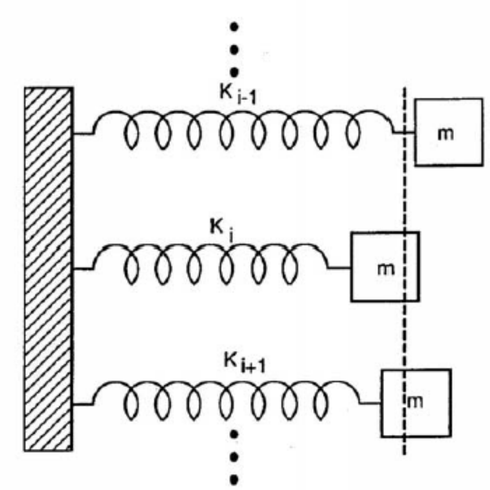


- Now the question is
  - Can we reduce the amplitude over time?
  - If yes, how quickly can we do it?

J. Marriner and D. McGinnis, AIP 249, 693 (1992)

# Stochastic Cooling

- With the kick, the change in amplitude is

$$\Delta x(t) = -g\bar{x}(t) = -\frac{g}{N}\sum_{i=1}^{N} x_i(t)$$

$$\Delta A_i^2(t) = \left[x_i(t) + \Delta x(t)\right]^2 - x_i^2(t)$$
$$= -2gx_i(t)\bar{x}(t) + g^2\bar{x}(t)^2$$
$$= -2gx_i(t)\frac{1}{N}\sum_{j=1}^{N} x_j(t) + \frac{g^2}{N^2}\sum_{j=1}^{N}\sum_{k=1}^{N} x_j(t)x_k(t).$$

- Averaging over time

$$\left\langle \Delta A_i^2(t,\tau)\right\rangle = \lim_{T\to\infty}\frac{1}{2T}\int_{-T}^{T}\left[-2g\underline{x_i(t+\tau)}\frac{1}{N}\sum_{j=1}^{N}\underline{x_j(t+\tau)} + \frac{g^2}{N^2}\sum_{j=1}^{N}\sum_{k=1}^{N}\underline{x_j(t+\tau)}\underline{x_k(t+\tau)}\right]d\tau$$

$$x_i(t+\tau) = A_i(t)\cos[\omega_i(t+\tau) + \phi_i]$$

J. Marriner and D. McGinnis, AIP 249, 693 (1992)

# Stochastic Cooling

$$\left\langle \Delta A_i^2(t,\tau)\right\rangle = \lim_{T\to\infty}\frac{1}{2T}\int_{-T}^{T}\left[-2g x_i(t+\tau)\frac{1}{N}\sum_{j=1}^{N}x_j(t+\tau)+\frac{g^2}{N^2}\sum_{j=1}^{N}\sum_{k=1}^{N}x_j(t+\tau)x_k(t+\tau)\right]d\tau$$

- Both terms on the right have

$$\frac{1}{2T}\int_{-T}^{T}x_i(t)x_j(t)dt = \frac{1}{2T}\int_{-T}^{T}A_i\cos(\omega_i t+\phi_i)A_j\cos[\omega_j(t+\tau)+\phi_j]dt$$

$$=\frac{1}{2T}\frac{A_iA_j}{2}\int_{-T}^{T}\cancel{\cos[(\omega_i+\omega_j)t+\phi_i+\phi_j]}+\cos[(\omega_i-\omega_j)t+\phi_i-\phi_j]dt$$

$$=\begin{cases}A_i^2/2, i=j\\ 0, i\neq j\end{cases}$$

- Therefore

Kick by self signal

$$\boxed{\left\langle \Delta A_i^2(t,\tau)\right\rangle} = -\boxed{\frac{2g}{N}\frac{A_i^2(t)}{2}}+\boxed{\frac{g^2}{N^2}\sum_{j=1}^{N}\frac{A_j^2(t)}{2}}$$

Amplitude change as a function of time

Kick by other signals other particles

J. Marriner and D. McGinnis, AIP 249, 693 (1992)

# Stochastic Cooling

$$\left\langle \Delta A_i^2(t,\tau)\right\rangle = -\frac{2g}{N}\frac{A_i^2(t)}{2} + \frac{g^2}{N^2}\sum_{j=1}^{N}\frac{A_j^2(t)}{2}$$

- Use $\sigma^2(t) = \left\langle \overline{x^2}(t)\right\rangle = \frac{1}{2N}\sum_{i=1}^{N} A_i^2(t),\ \Delta\sigma^2(t) = \frac{1}{2N}\sum_{i=1}^{N}\left\langle \Delta A_i^2(t,\tau)\right\rangle,$ and summing over $i$, we have

$$\sum_{i=1}^{N}\left\langle \Delta A_i^2(t,\tau)\right\rangle = -\frac{2g}{N}\sum_{i=1}^{N}\frac{A_i^2(t)}{2} + \frac{g^2}{N^2}\sum_{i=1}^{N}\sum_{j=1}^{N}\frac{A_j^2(t)}{2}$$

$$\Delta\sigma^2(t) = \frac{-2g+g^2}{N}\sigma^2(t)$$

- That is, the average amplitude changes over time!
- Can be cooling or heating! At optimum gain $g_0=1$,

$$\Delta\sigma^2(t) = -\frac{1}{N}\sigma^2(t)$$

- This is the change per correction.
- That favors smaller particle numbers!

J. Marriner and D. McGinnis, AIP 249, 693 (1992)

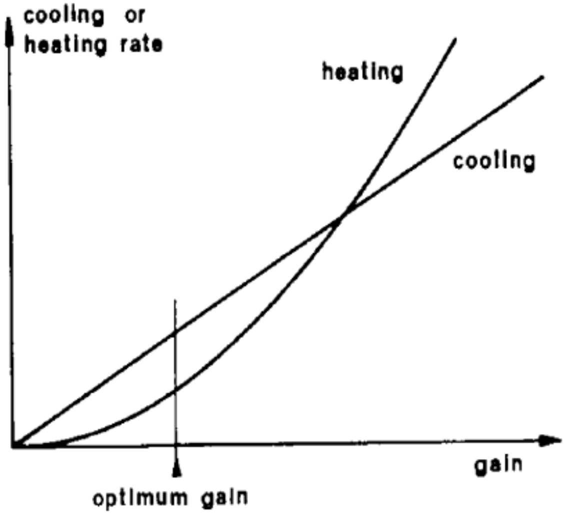


S. Van der Meer, Nobel prize talk

# Optical Stochastic Cooling

the change per correction, at optimum gain, is

$$\Delta\sigma^2(t) = -\frac{1}{N}\sigma^2(t)$$

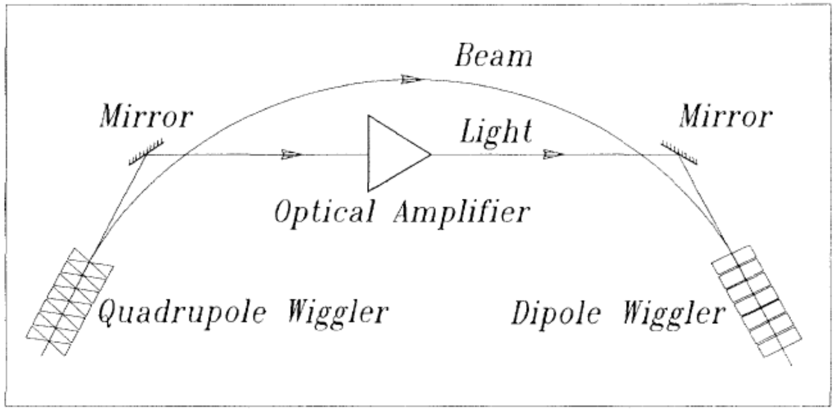


with a gain bandwidth of $\Delta f$, we can make $\Delta f$ measurements/corrections per sec

$$\frac{d\sigma^2(t)}{dt} = -\frac{\Delta f}{MN}\sigma^2(t)$$

where M is a mixing parameter (M=1 perfect mixing after each pass, M>1 imperfect)

Cooling time $\tau$ estimate

$$\frac{\tau}{T} \cong \frac{N}{\Delta f}(c/l_b) \approx 2N_u$$

$\tau$ : cooling time, $c$ : spd of light

$T$ : rev period, $l_b$ : bunch length

$N$ : # part.in bunch

$N_u$ : # in bandwidth

Bandwidth in microwave systems limited to GHz (~8) regime. With an optical amplifier bandwidths are in the THz regime. This is the motivation for Optical Stochastic Cooling

$$\lambda = 1\,\mu\text{m} \Leftrightarrow \nu = 300\,\text{THz}$$

$$\text{if } \frac{\Delta\nu}{\nu} = 10\%,\ \Delta\nu = 30\,\text{THz}$$

Michailichenko & Zolotorev PRL 71, 4146 (1993)

# Optical Stochastic Cooling

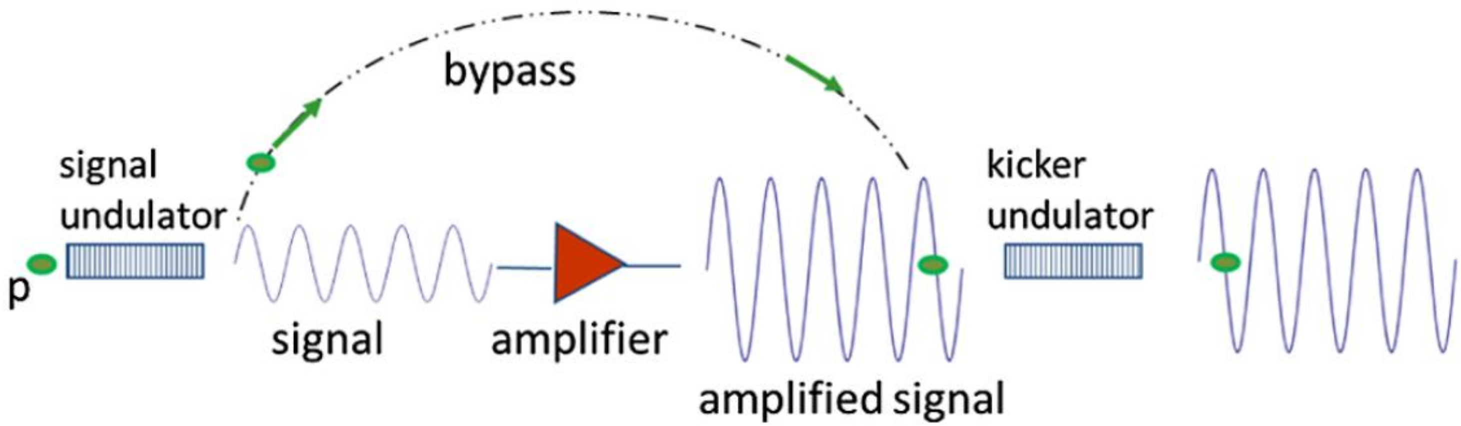


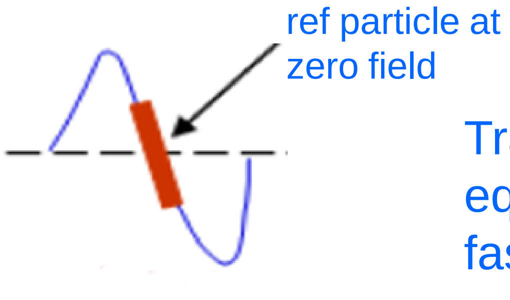


Transit-time cooling: tune bypass so that particle with the equilibrium momentum arrives at zero-field, and faster/slower arrive around it.

Issues:
- for hadrons, radiation is weak and required amplified power is large
- very large wiggler fields required (~10T)
- diagnostics (long cooling times)

# Optical Stochastic Cooling: RHIC proposal

For a fixed cooling time, the required optical amplifier power scales as

$$P \prec \lambda^{-1}$$ go to longer wavelength

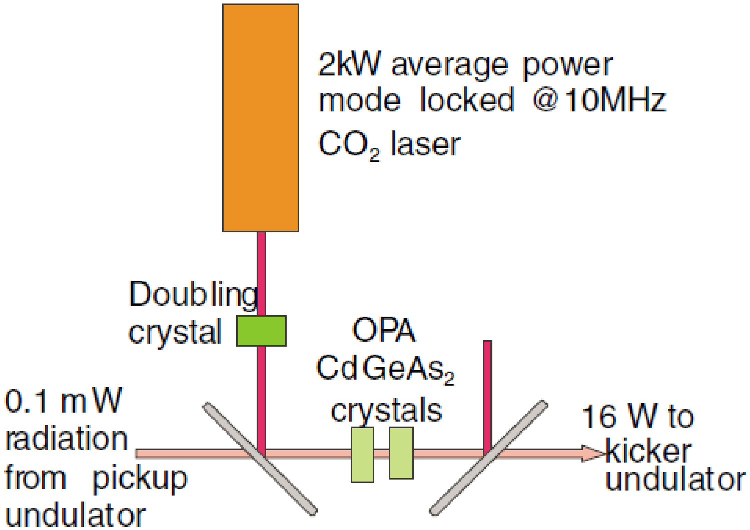


OPA gain curve

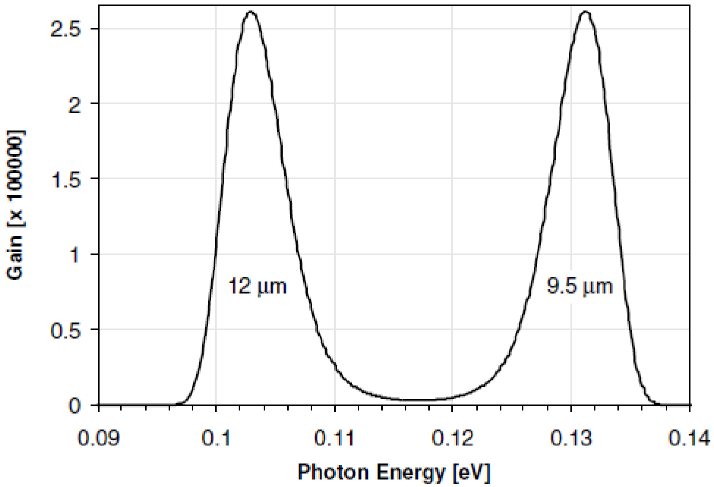


Babzien et al PRSTAB 7, 012801 (2004)

- frequency-doubled CO2 laser pumping a CdGeAs2 OPA
- gain of 2.5 x $10^5$ at 12 um
- 6% bandwidth: 1.5 THz
- 1 hour damping time for N=$10^9$ bunches of Au ions

# OSC: MIT proposal, use electrons

- Demonstration of OSC with electrons can point way to cooling beams at very high energy and high bunch population
  - OSC of electrons much faster (seconds) than for hadron beams (hours)
  - Modest technical requirements (wiggler, amplifier, bypass chicane)
  - Develop techniques and diagnostics needed to achieve OSC in practice
  - Evaluate prospects for OSC in high-energy, high-brightness regimes
- Broadband optical parametric amplifier (developed by MIT-RLE)
  - Large dispersion-free linear amplification in short medium
  - Total delay ~20 ps with control to a fraction of an optical cycle
- Small angle (65 mrad) OSC bypass with 6 mm path length change makes the setup robust
  - Fixed optics with achievable magnet tolerances
  - Minimize effects of synchrotron radiation and required changes to SHR RF
- Undulators matched to amplifier wavelength (2 $\mu$m), bandwidth (~10%)
- All readily integrated within 10 m of SHR east straight section

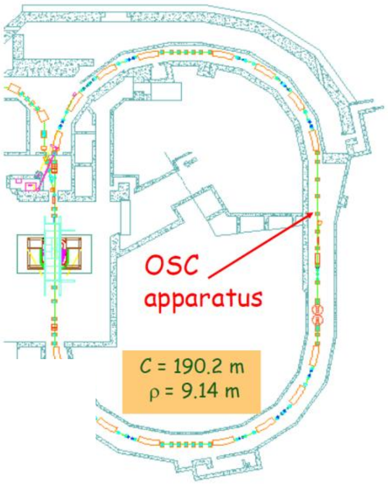


South Hall Ring (SHR)

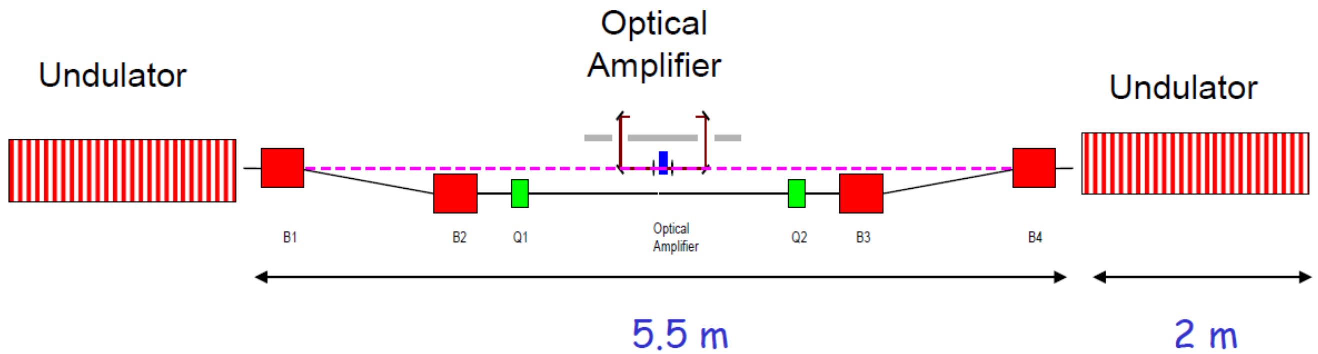




W Barletta et al, EICAC 2009
www.jlab.org/conferences/eicac/OSC-EICAC.pdf

# MIT proposal, optical amplifier

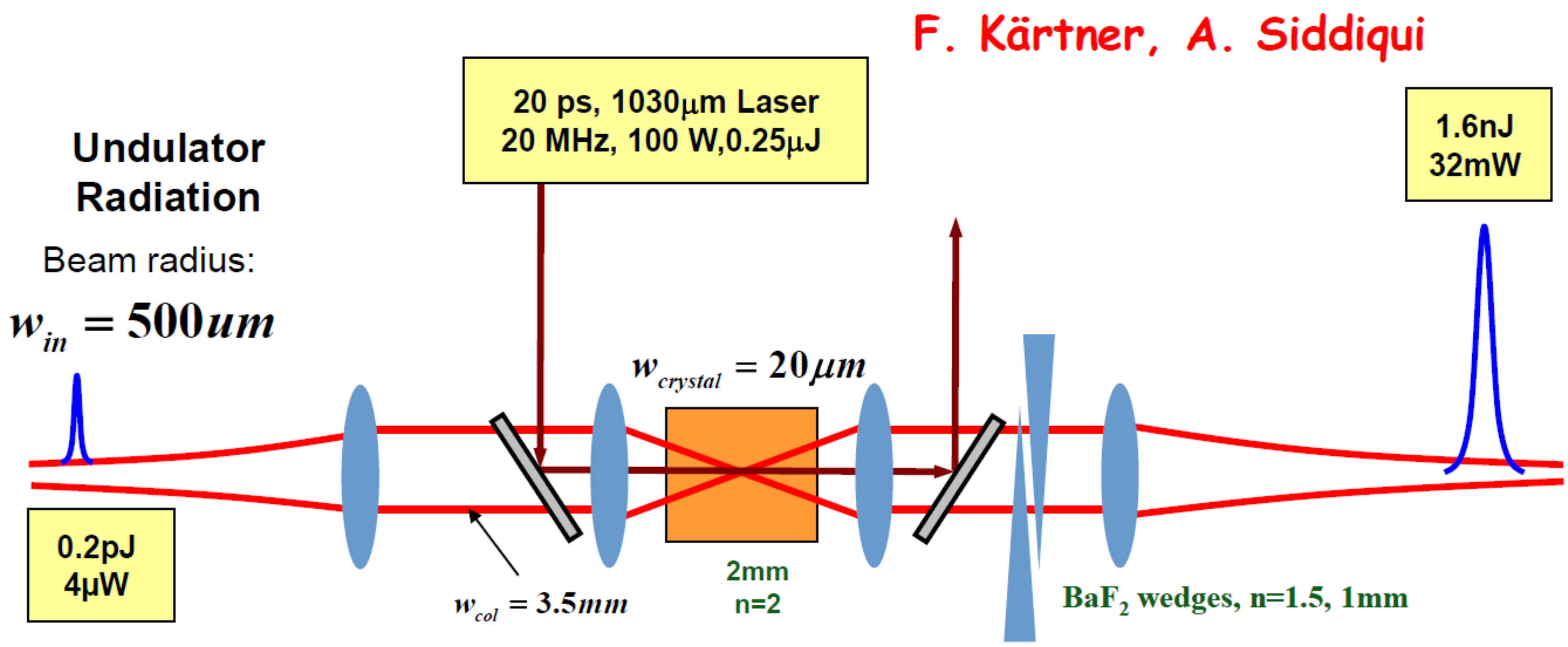


- Amplification in periodically poled lithium niobate crystal (PPLN)
- Pump laser controls gain; phase-locked to stored electron beam
- Optics internal to SHR vacuum system; remotely actuated
- Fine phase control allows interferometry in 2nd undulator for achieving OSC

W Barletta et al, EICAC 2009
www.jlab.org/conferences/eicac/OSC-EICAC.pdf

# Optical Stochastic Cooling: planned FNAL test

Study for potential application in LHC

## IOTA – Test ring for Non-Linear Optics and Optical Stochastic Cooling

- Small test ring in NML building
- It is planned to test both OSC scenarios: with and without optical amplifier
- ASTA injector (~20 MeV) would be sufficient for filling the ring

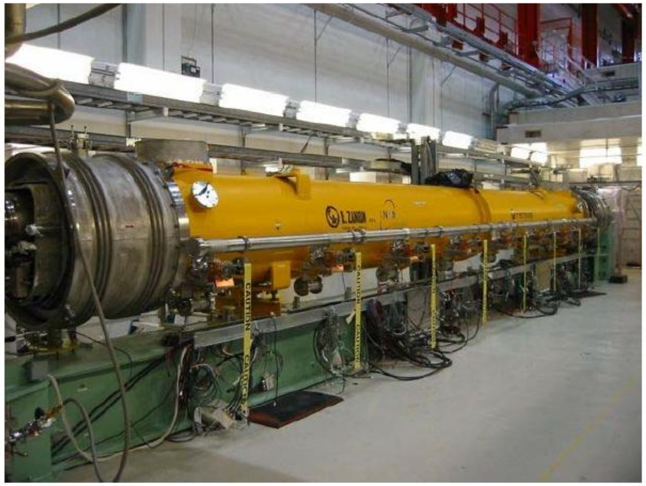

SC 1.3 GHz linac

Empty room for IOTA

Optical stochastic cooling, Valeri Lebedev, July. 27, 2012

Valeri Lebedev FNAL seminar, July 2012

# Coherent Electron Cooling

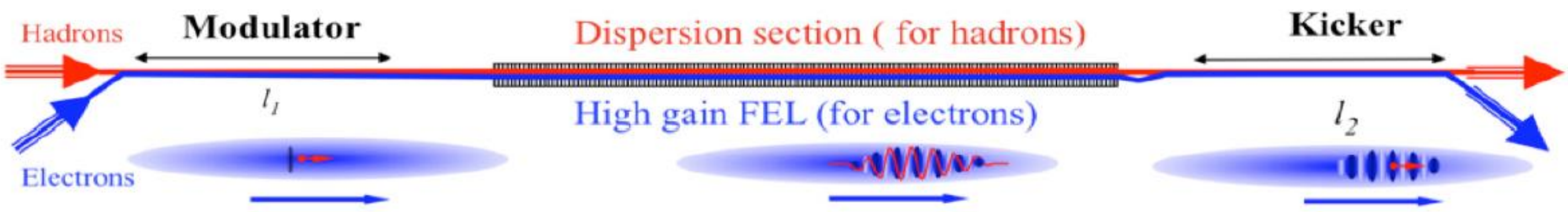


Litvinenko et al IPAC 11 THPS009

Not really a laser manipulation of a beam, but related to other schemes in this section

- technically, you could argue a beam is manipulated *inside* the laser (FEL)

- e-beam and hadron beam are overlapped in 'modulator' section
- e-beam density is modulated by hadrons (Debye screening)
- density modulation is amplified inside of the FEL
- amplified density modulation is phase-shifted relative to hadron beam in kicker so that hadrons receive kicks from electrons towards their central velocity
- Proof of principle test under construction at BNL/RHIC

# FEL seeding with High Harmonics

## What is HHG?

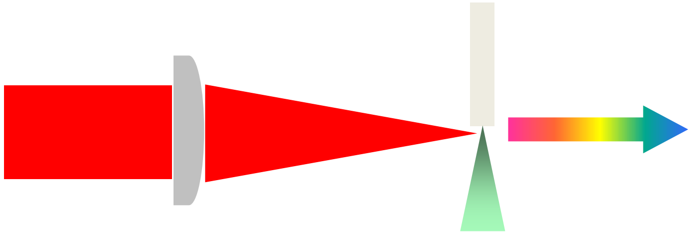

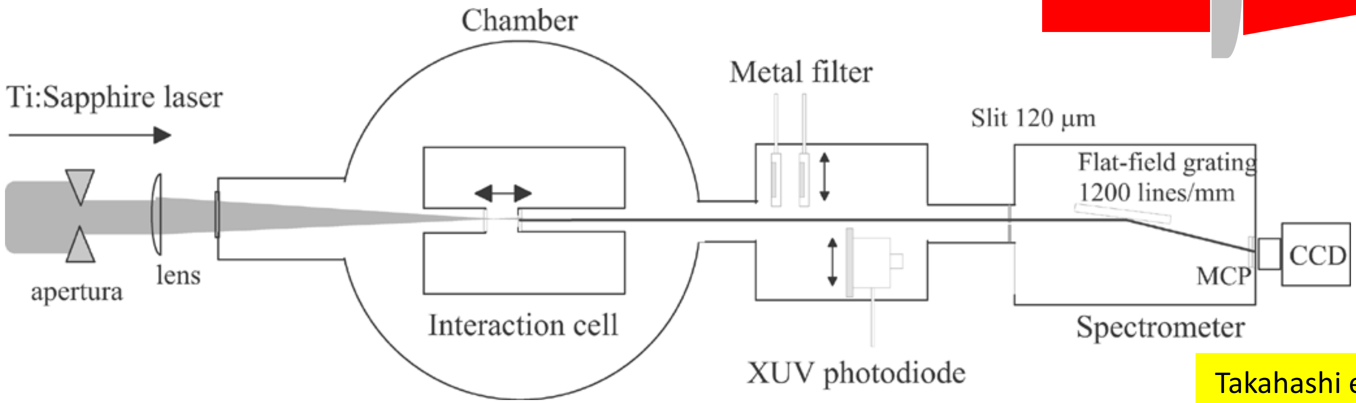


Takahashi et al, IEEE JQE 10,1315 (2004)

Ultrafast pulse focused into a gas sample

- Xe, Ar, Ne, He
- Intensity ~ $10^{14} – 10^{15}$ W/cm$^2$
    - ionization plays a role both in quenching (saturation) & phase-matching
- sample may be in a jet, capillary (waveguide) , or cell
    - phase matching
- Cutoff is intensity- and atom-dependent

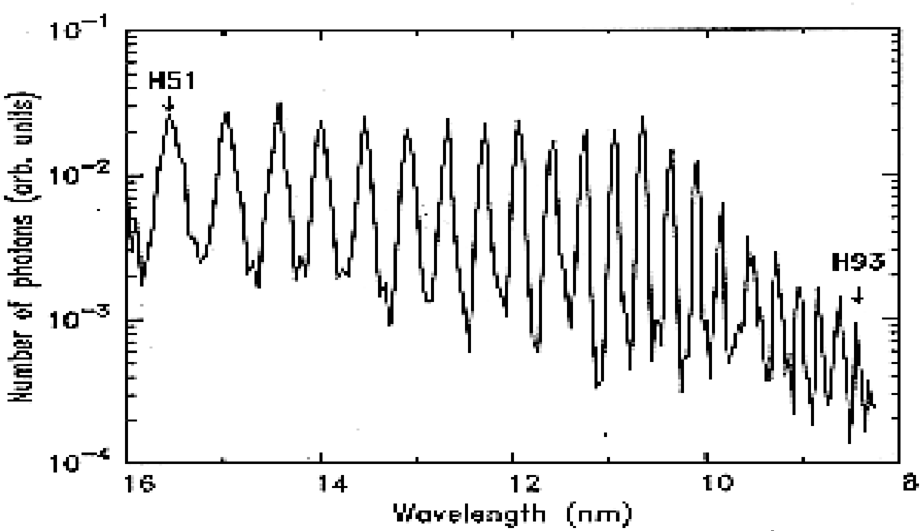


Helium, 800 nm L'Huillier et al, Lund

# FEL seeding with High Harmonics

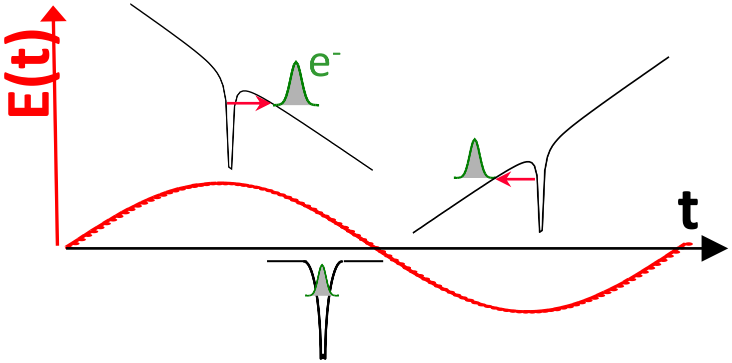


**The Three-Step Model**
Kulander, Schafer, and Krause *SILAP III* (1993)
P. Corkum, Phys. Rev. Lett. 71, 1994 (1993).

Optical Field Ionization

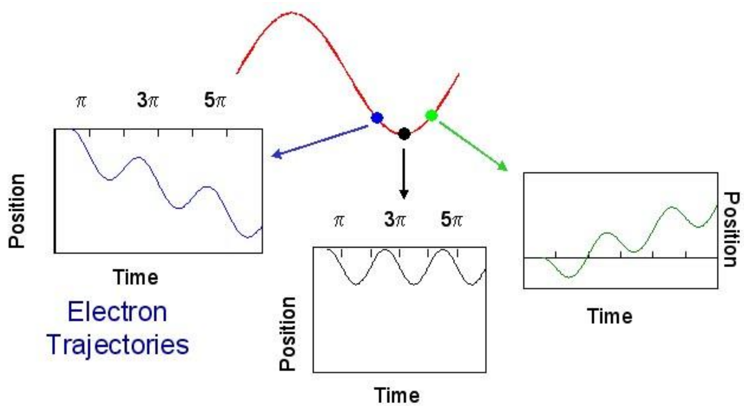


Free electron moving in the optical field.
Its average kinetic energy is $U_p$, a scaling parameter of the dynamics

$$U_p = \frac{e^2 E_o^2}{4 m_e \omega^2}$$

$$U_p \propto I\lambda^2$$

$$\approx 1\,\mathrm{eV}\ @\ I = 10^{13}\,\mathrm{W/cm^2},\ \lambda = 1.06\,\mu\mathrm{m}$$

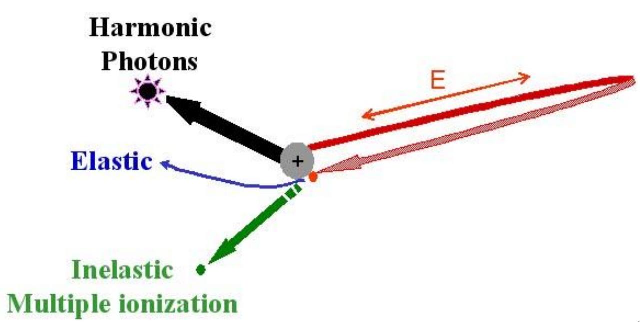


Some electrons return and interact with the core: HHG, MPI, multiple ionization

# FEL seeding with High Harmonics

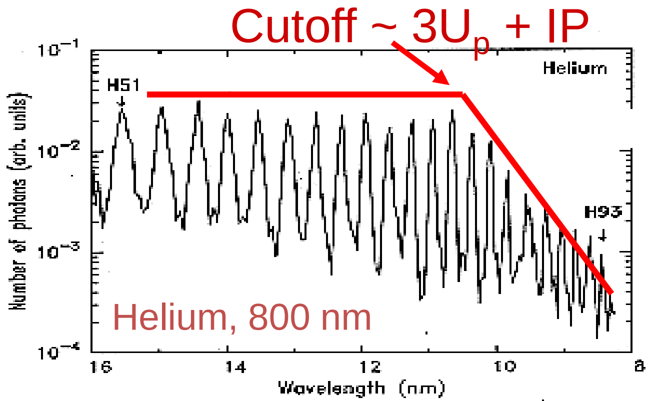


L'Huillier et al, Lund

Approximate cutoff position is given by classical mechanics*

*Shorter pulses non-adiabatic effects push cutoff higher

* ignoring macroscopic phase matching

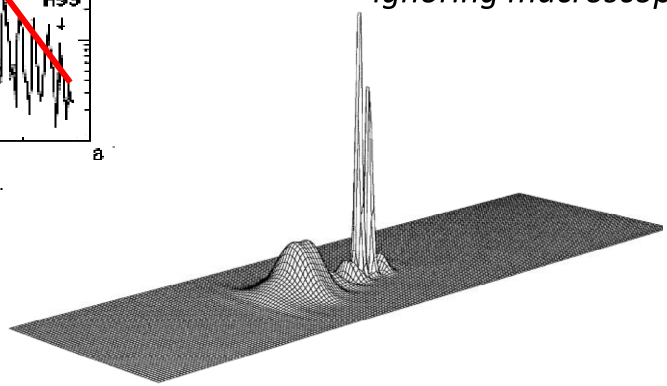

Quantum treatments:

- TDSE *Kulander, Schafer*
    - single electron, wave function propagation on grid
- *Gordon & Kaertner*
- Strong Field Approximation *Lewenstein*
    - ionization from simplified core
    - free electron propagation (in E field) outside of core
    - faster, complex polarizations, multiple frequencies
- Quantum Path Distributions/ Path Integral Formalism *Gaarde & Schafer, Salieres & Lewenstein*
    - insight into phase matching and time-frequency anaylsis

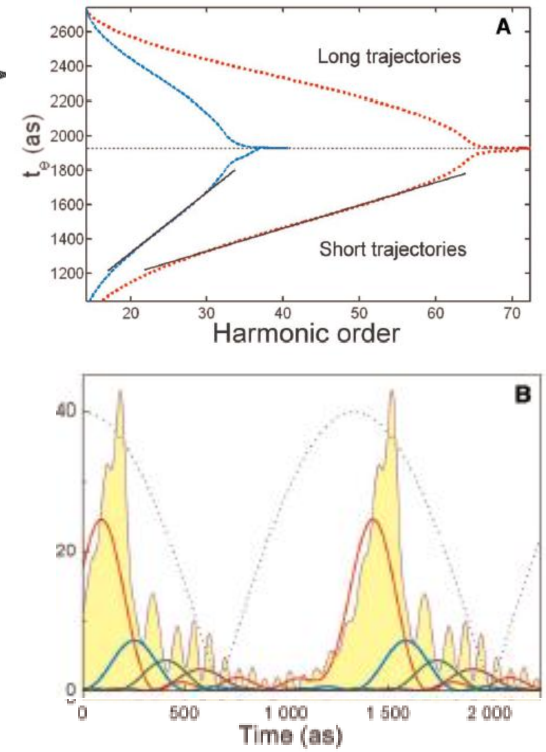


Mairesse et al Science 302, 1540 (2003)

# FEL seeding with High Harmonics

Attosecond Structure in the harmonics

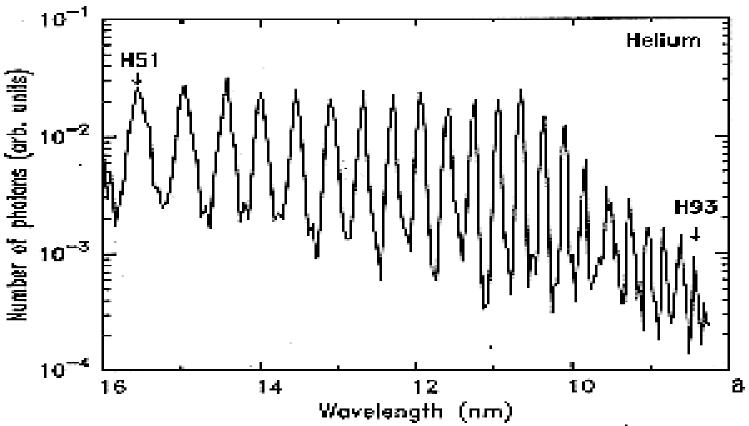


- Plateau electronics form a frequency comb
    - Well defined relative phases
    - attosecond pulse trains & attosecond pulses
- Emission time for harmonic groups distinguishable
    - chirped over the plateau

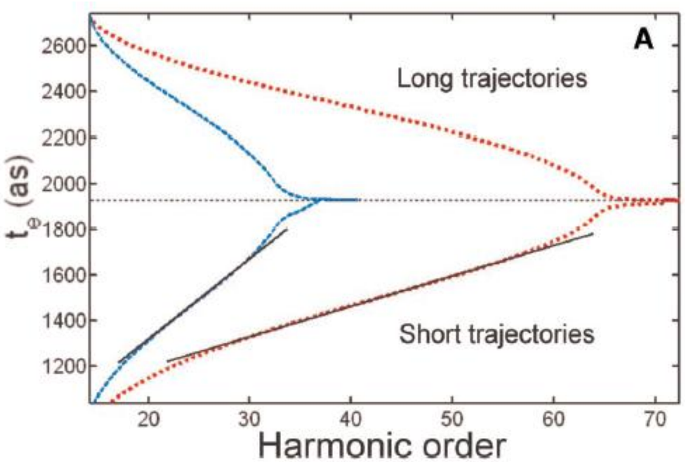


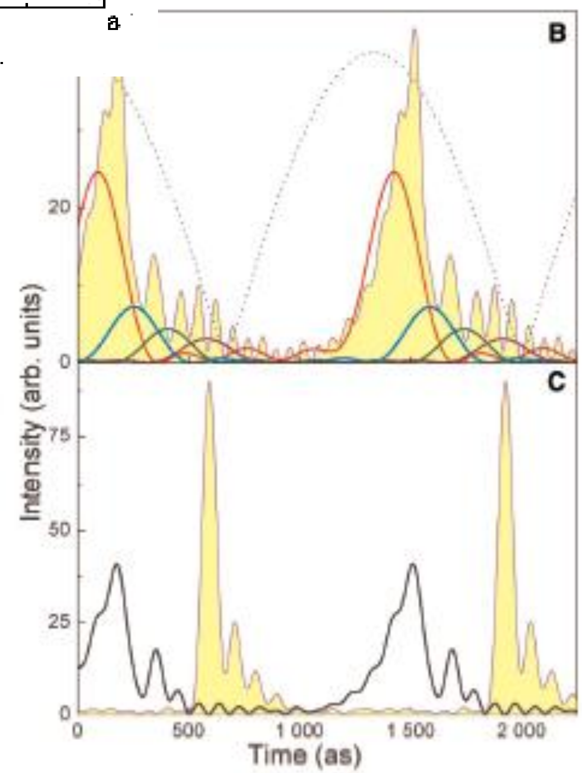


Mairesse et al Science 302, 1540 (2003)

# FEL seeding with High Harmonics

## Longer λ is Better for reaching higher harmonics

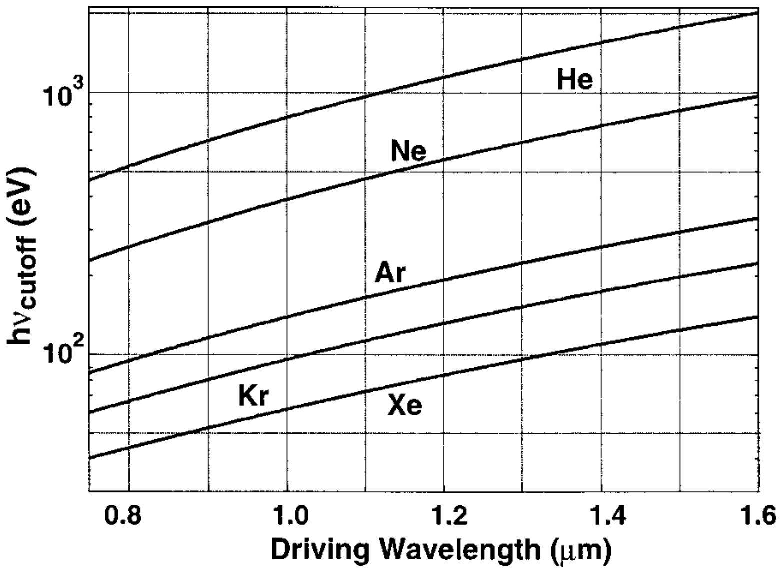


FIG. 1. Calculated relationship between single-atom HHG cutoff photon energy and the driving wavelength.
From Shan and Chang PRA **65** 011804 (2001)

Single atom efficiency at the harmonic cutoff, effect of fundamental wavelength

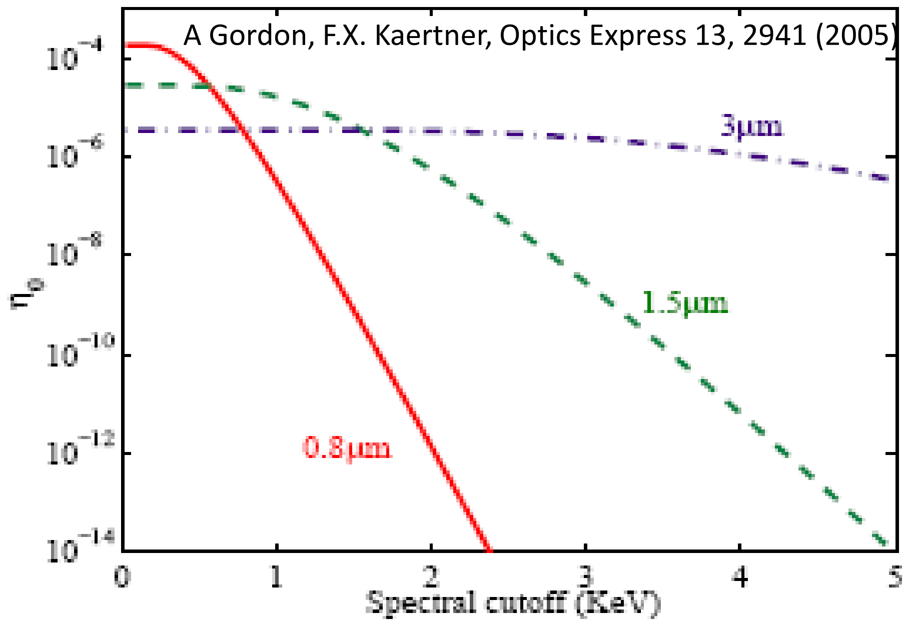


But Macroscopic phase matching effect also important and wavelength dependent circa 2006; ignore black & blue solid lines

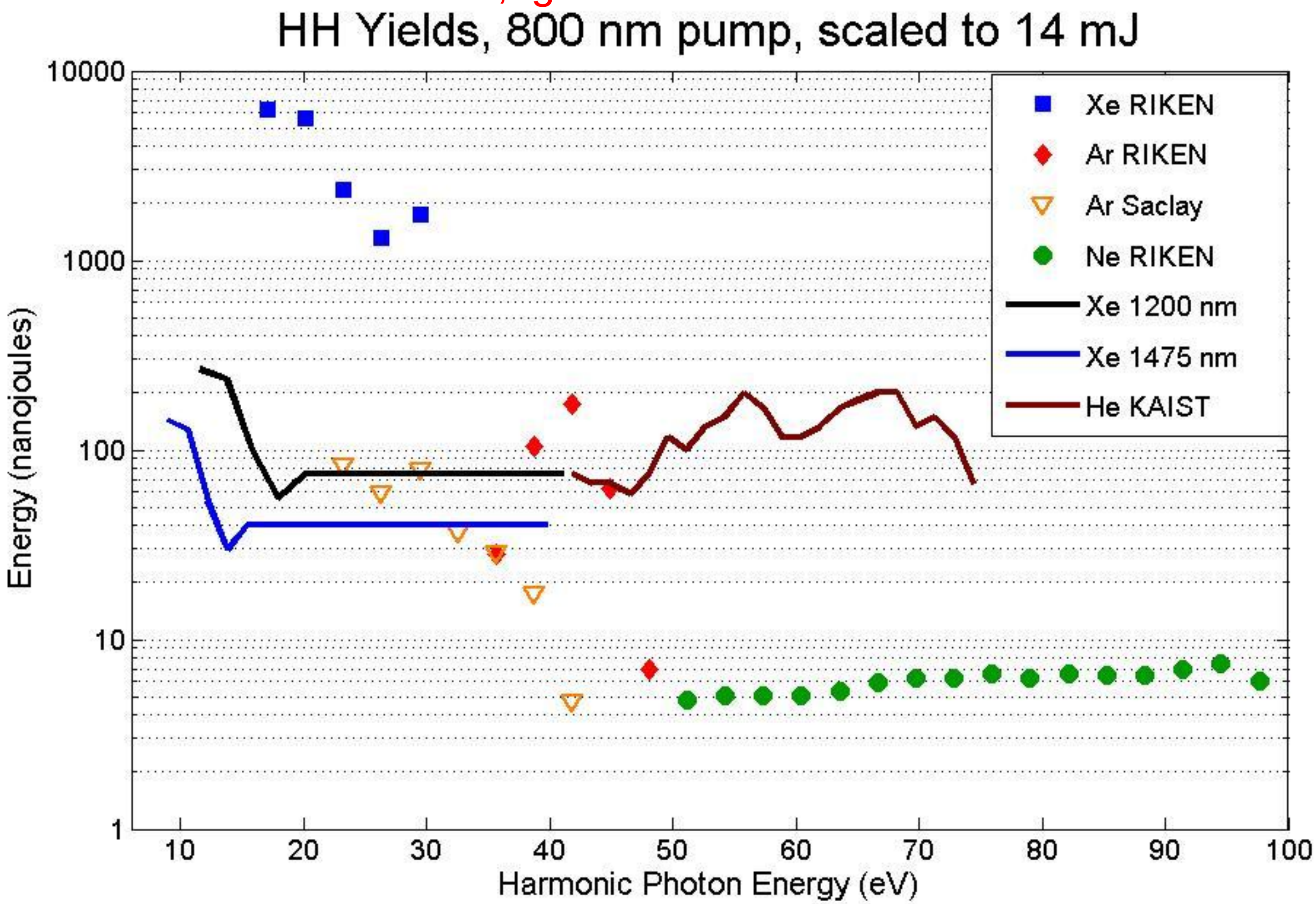

# Seeding of FEL with H5 from 800 nm pump @ SPring8

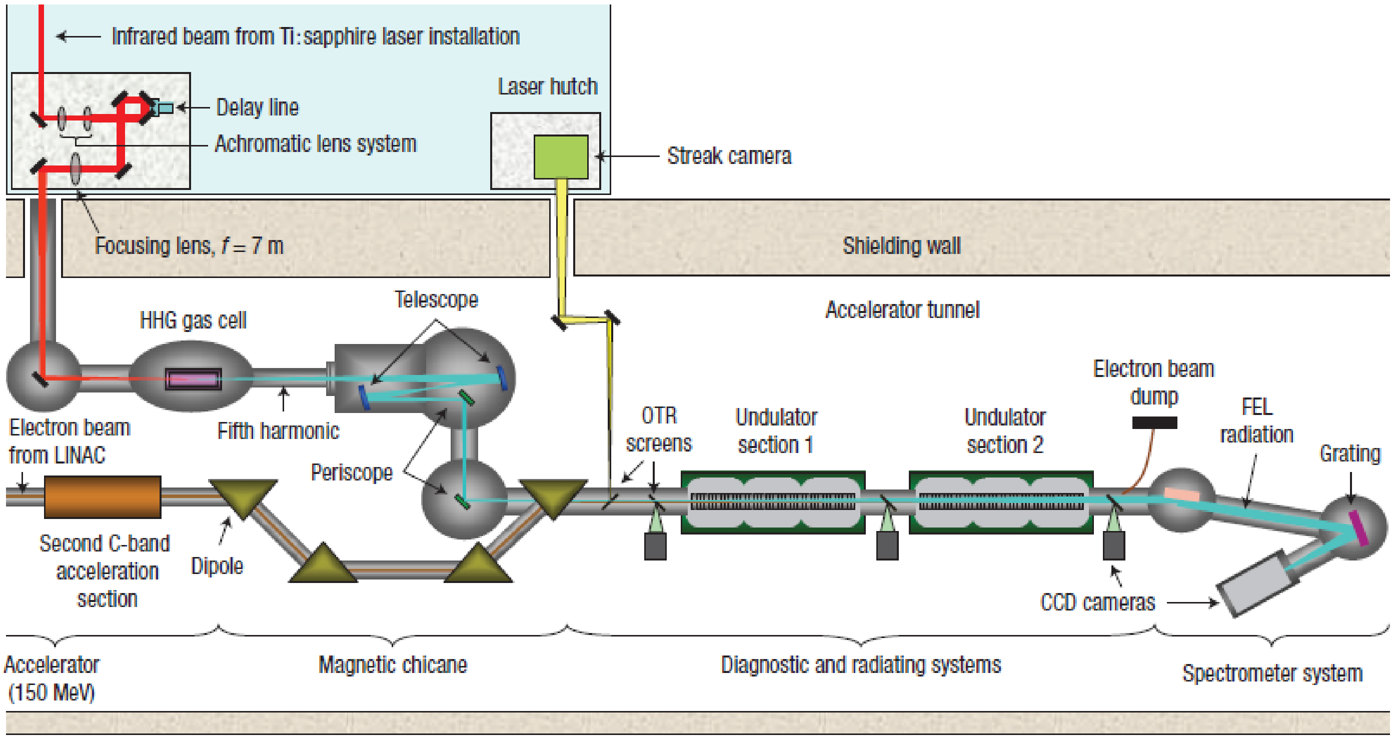


- $\lambda_L$= 800 nm, $\tau$ = 100 fs, 20 mJ, 10 Hz
- $\lambda_{H5}$=160 nm, $\tau \approx$ 50 fs, $E_{max} \approx$ 1 uJ, Xe gas cell
- e- beam: $\tau$ = 1 ps, E = 150 MeV, 10 Hz



Lambert et al Nature 4, 296 (2008)

# Seeding of FEL with H5 from 800 nm pump @ SPring8

First Undulator only, $E_{seed}$=0.53 nJ

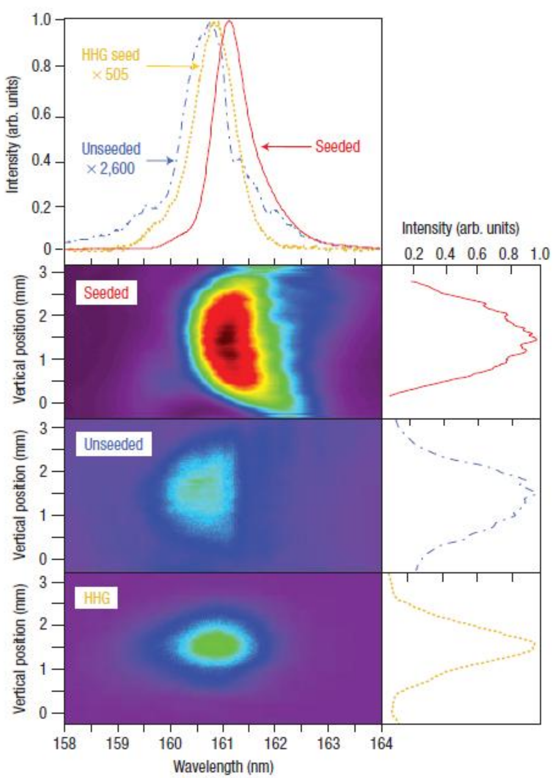


**Figure 2 Comparison between the FEL seeded emission, the unseeded emission and the HHG seed at the fundamental wavelength (160 nm).** The spatial (vertical) and spectral distributions are mapped on the CCD (charge-coupled device) camera of a spectrometer; spatial (right) and spectral (up) profiles are plotted at maximum intensity. The lines correspond to the seeded (single shot, line) and unseeded emission (averaged on 10 shots, dash–dot) and the HHG seed (single shot, dots). The seed pulse energy was 0.53 nJ and only the first undulator section was used for amplifying the HHG pulse.

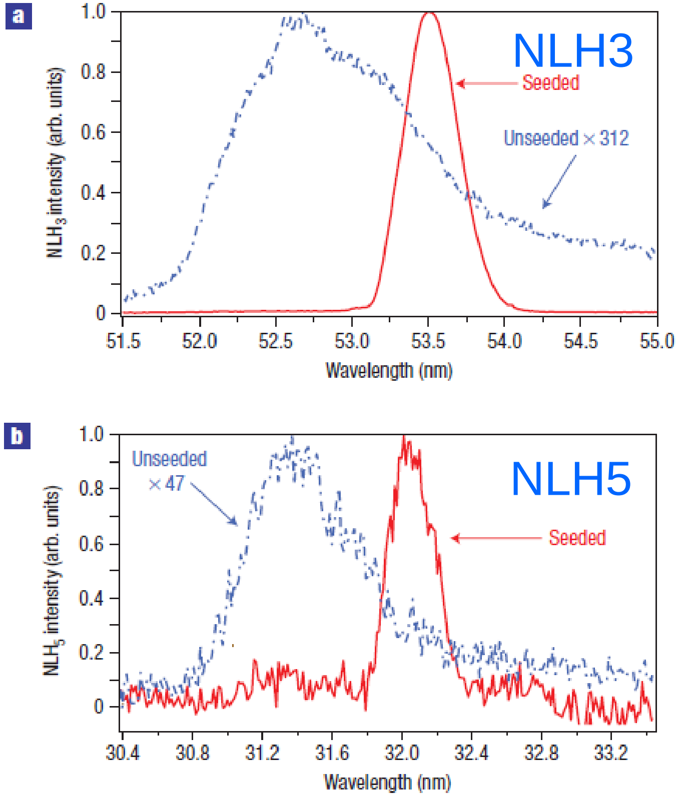


**Figure 3 Spectra of the FEL seeded and unseeded emission at the wavelengths of the third and fifth NLHs.** The spectra have been obtained by integrating the two-dimensional distributions of the CCD images (as for Fig. 2) over the vertical dimension. The seeded (single shot, line) and unseeded (averaged on 10 shots, dash–dot) FEL emissions are plotted for the third (**a**) and fifth (**b**) NLHs. The seed pulse energy was 0.53 nJ and only the first undulator section was used for radiating the NLHs.

Lambert et al Nature 4, 296 (2008)

# Seeding of FEL with H5 from 800 nm pump @ SPring8

1 & 2 undulators

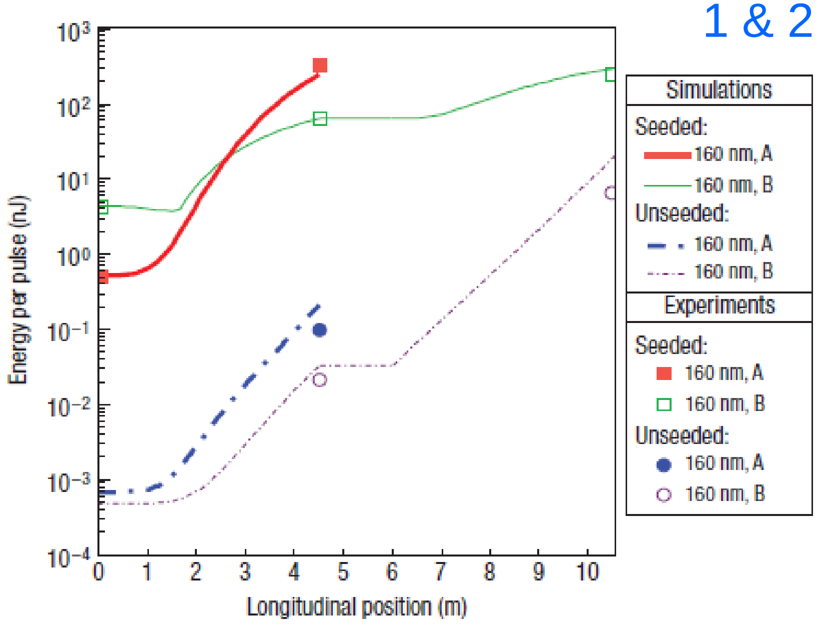


**Figure 4 Evolution of the 160 nm FEL pulse energy along the two undulator sections: comparison of experimental data and simulations using PTD code.** The two sections, each of 4.5 m, are separated by a 1.5-m-long drift space. Two cases of amplification are considered, at low and high HHG seed energy, respectively; they also differ slightly in the electron-beam brightness and the spatial/spectral overlaps between the seed and electron beam.

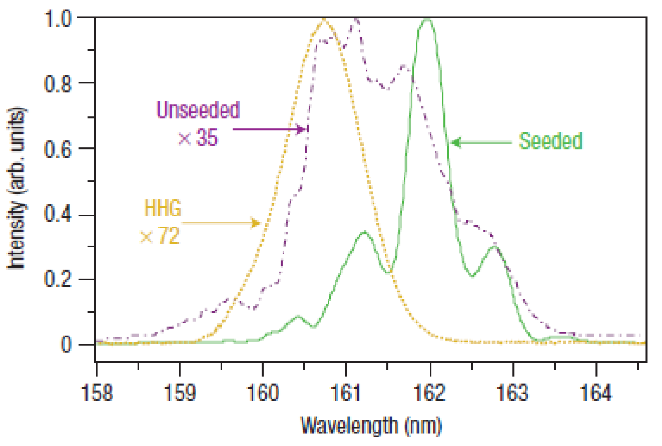


**Figure 5 Spectra of the FEL fundamental emission using the two undulator sections:** unseeded (single shot, dash–dot) and seeded (single shot, line) obtained with a 4.3 nJ seed (single shot, dots). The FEL gain is smaller compared with the measurements in Figs 2 and 3, because of the lower electron-beam brightness ($B_p < 200$ A ($\pi$ mm mrad)$^{-2}$), transverse misalignment ($F_f < 1$) and spectral detuning ($\lambda_{seed} - \lambda_{SE} \leq 0$).

Case A: 0.53 nJ seed, $F_f$ =1, lseed−$l_{SE}$ = 160.85−160.72=0.13 nm, $B_p \approx 200$ A ( $\pi$ mm mrad)$^{-2}$.

Case B: 4.3 nJ seed, $F_f$ =0.4, lseed− $l_{SE}$ = 160.84−160.98=−0.14 nm, $B_p \approx 180$ A ( $\pi$ mm mrad)$^{-2}$

Points are experimental data; lines are calculations for the same conditions.

- SASE unsaturated
- seeded is oversaturated
- spectral narrowing agrees with simulation results (Perseo, GENESIS)
- nanoJoule seed levels sufficient
- nonlinear harmonics strongly enhanced

Lambert et al Nature 4, 296 (2008)

# Seeding of FEL with H13 from 800 nm pump @ SPring8

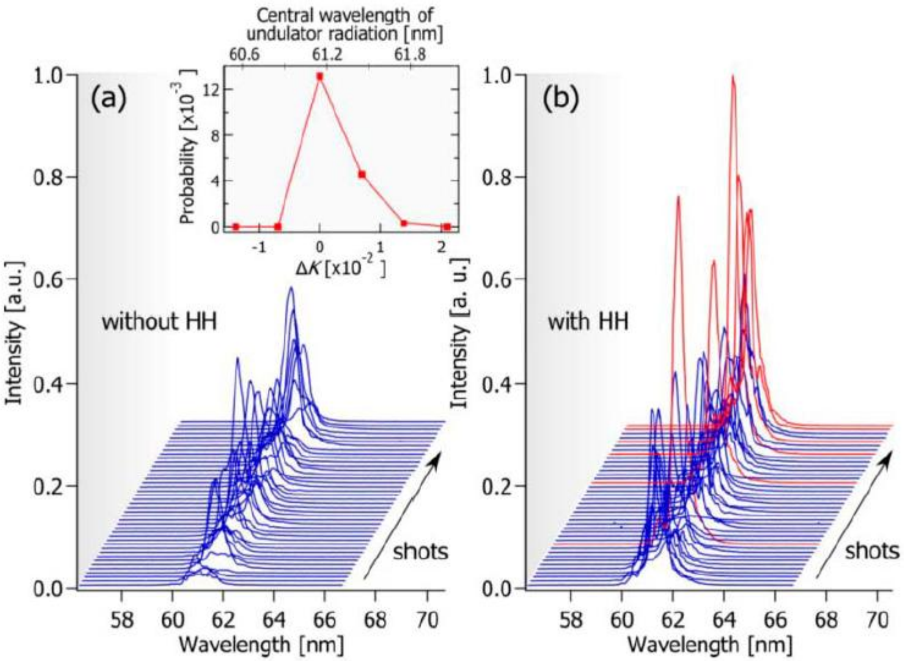


Fig. 2. Spectra of FEL radiation in fifty successive shots without (a) and with (b) HH injection. The red lines in (b) show profiles that have higher intensities above the threshold level. The inset shows an appearance probability of the high-intensity condition as a function of the deviation of K-value, $\Delta K = K$-1.37944 (lower axis), and the central wavelength of the undulator radiation (upper axis).

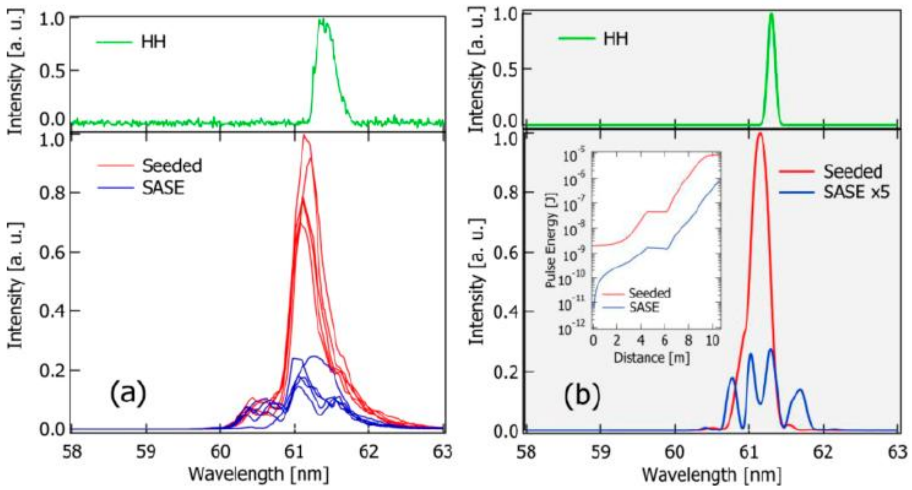


Fig. 3. Spectra of seeded (red lines) and unseeded (blue lines) conditions, as well as that of HH radiation (green line), given by experiment (a) and simulation (b). The inset of (b) shows intensity growths along the undulator for seeded (red line) and unseeded (blue line) conditions.

- Experiment complicated by jitter problems
- gain of 650 from estimated seed energy
- estimated 2 nJ seed energy sufficient

Togashi et al Opt Exp 19, 317 (2011)

# Enhanced-Current Self-Amplified Spontaneous Emission (ESASE)

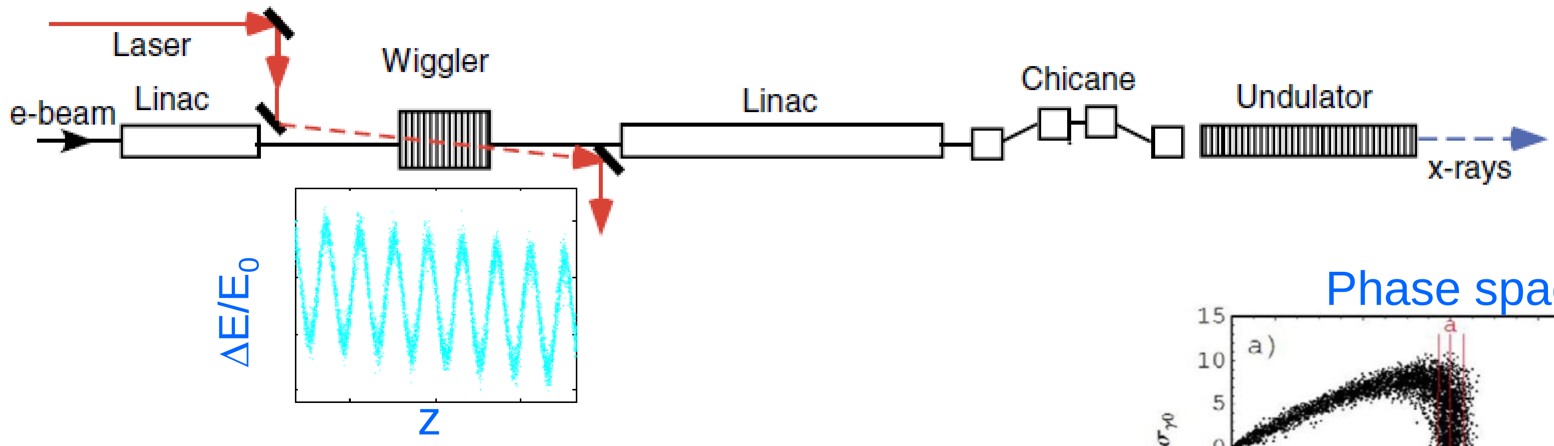


- overlap IR pulse with short section of the electron bunch in the modulator
  - modulate $e^-$ energy at optical period
  - minimal density modulation
- after acceleration, chicane converts energy modulation into density modulation
- current spikes 100s of attoseconds long at optical period
- gain length in current spikes << gain length elsewhere
  - attosecond SASE dominates
- SASE intrinsically synchronized with modulating laser

Phase space

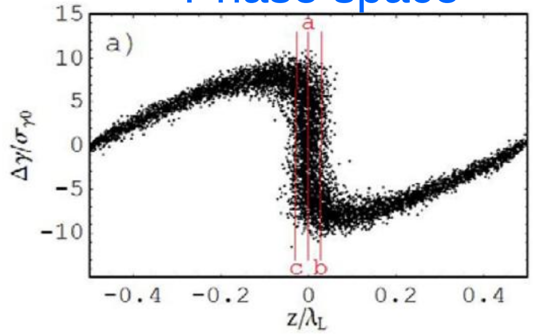


Current

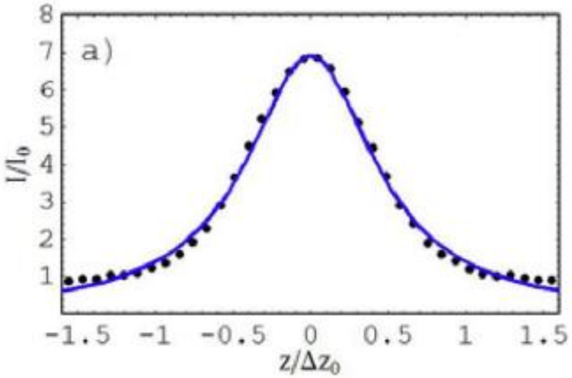


Zholents PRL 8 040701 (2005)

# ESASE

• for a rectangular pulse in a wiggler with $N_w$ periods, the amplitude of the modulation $\Delta\gamma_w$ is given by

$$\Delta\gamma_w^2 = 33\pi \frac{P_L}{P_A} N_w \xi_w [J_0(\xi_w/2) - J_1(\xi_w/2)]^2$$

$$P_A = I_A mc^2/e \approx 8.7 \text{ GW}, \quad I_A = 17 \text{ kA} \quad \xi_w = K_w^2/(2+K_w^2)$$

$$K_w = eB_w\lambda_w/(2\pi mc)$$

• laser power scale given by $P_A$ is 9 GW, so need an ultrafast laser
• need to reach B ≡ $\Delta\gamma_W/\sigma_{\gamma 0}$ values of 5-10, where $\sigma_{\gamma 0}$ is the uncorrelated energy spread of the electrons
• after the chicane, the current microbunches have widths

$$\boxed{\Delta z_0 = \lambda_L/2B}$$

• so for B~5, you get current spikes an order of magnitude shorter than an optical wavelength, repeated at the optical period (just one spike shown)

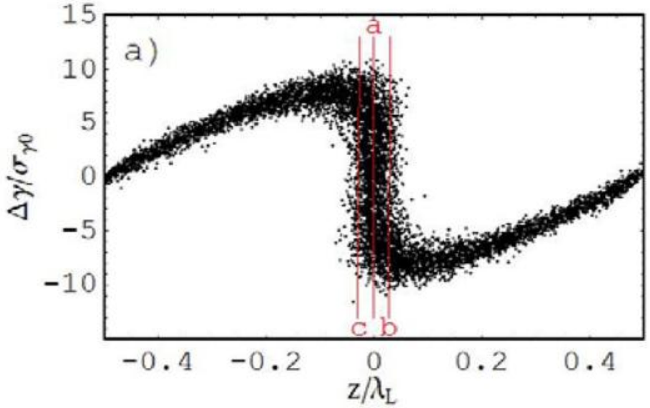


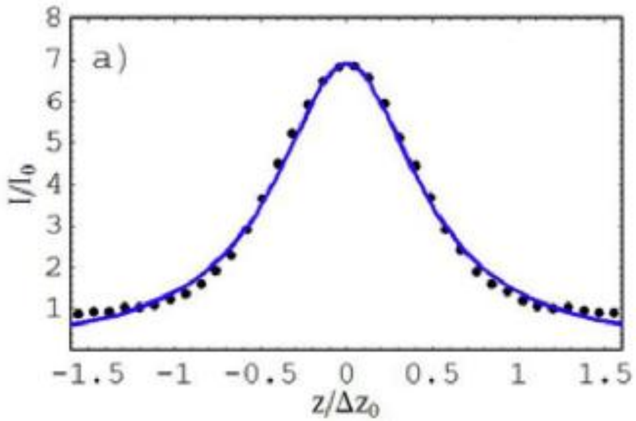




Zholents PRL 8 040701 (2005)

# illustration of how B impacts $\Delta z_0$:

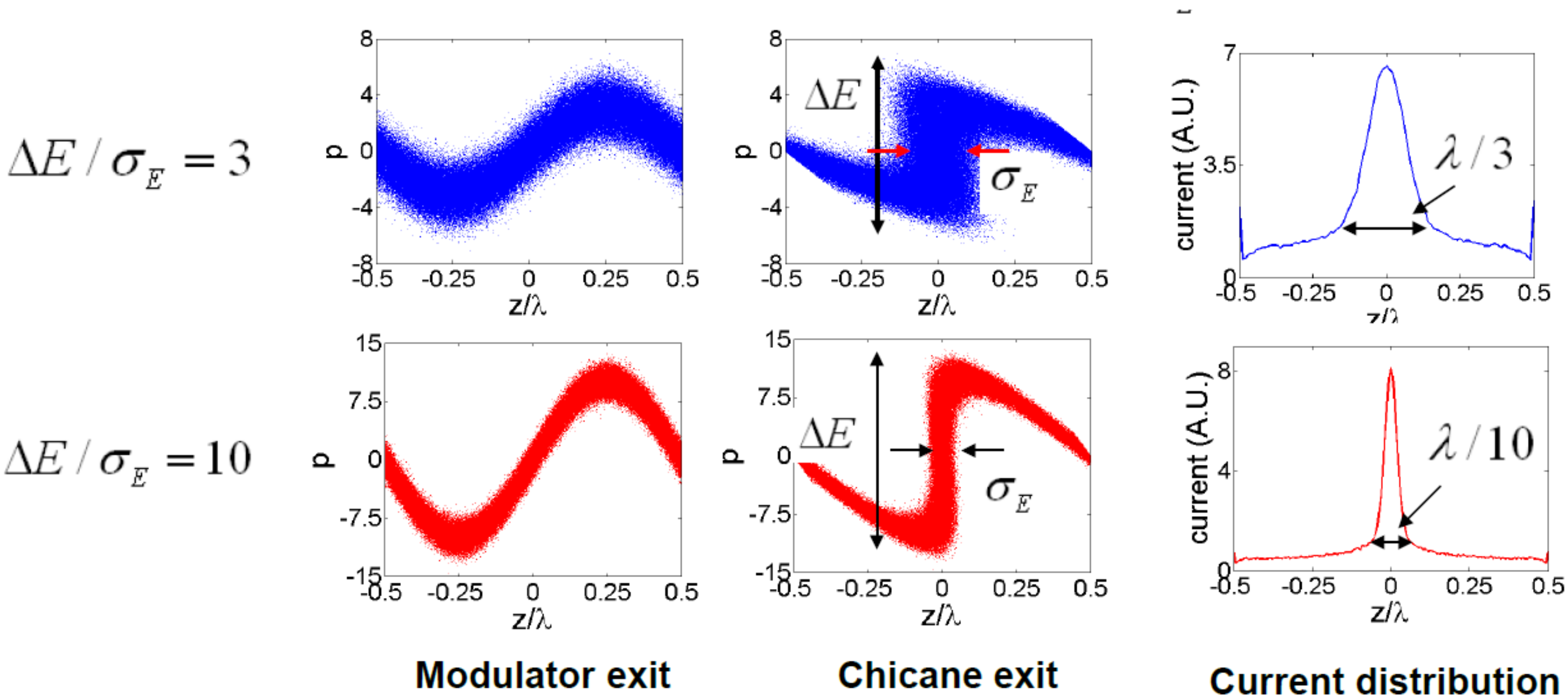


pic from Dao Xiang's PAC'11 talk on EEHG

# ESASE

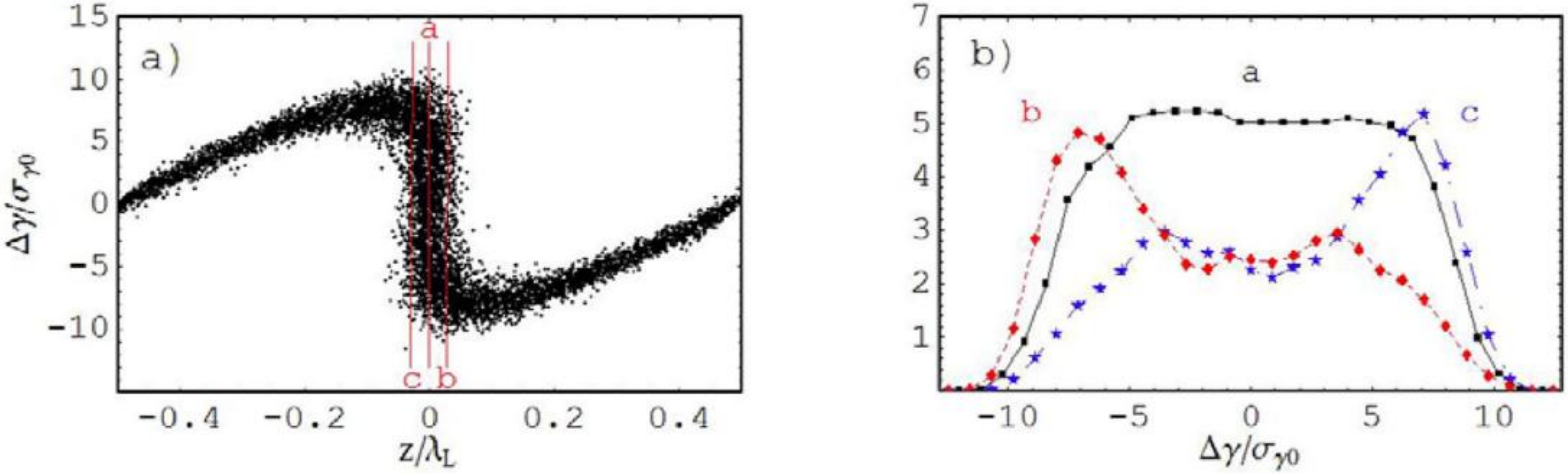


amplitude gain length in wiggler periods (~$8M_G$ to saturation)

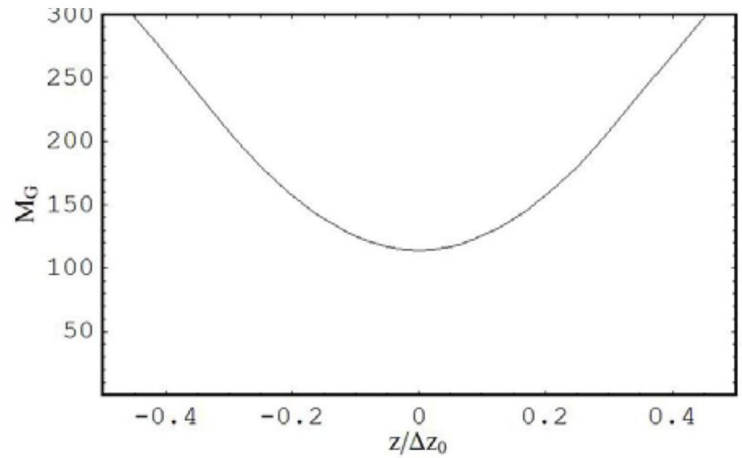


- The energy distribution favors lasing in the central part of $\Delta z_0$, further reducing the width of the SASE radiation



Zholents PRL 8 040701 (2005)

# ESASE

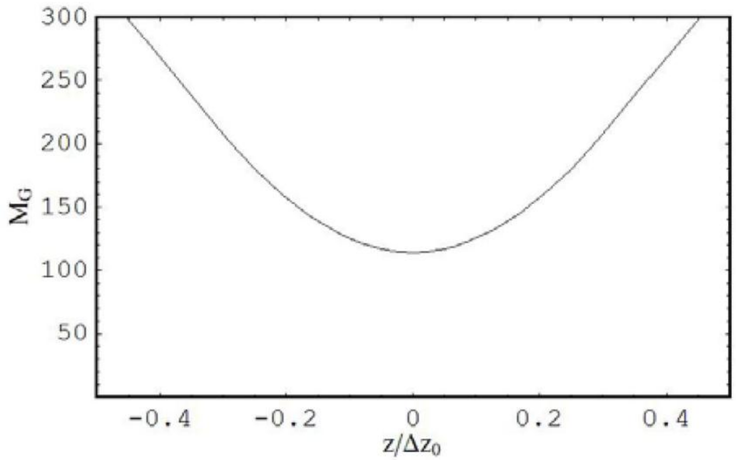


This also constrains the laser wavelength:  You need the slippage over the saturation length to be less than the length of the current spike (recall the slippage is one output wavelength $\lambda_x$ per radiator wiggler period):

$$z0 = \frac{\lambda_L}{2B} > 8M_G\lambda_x \quad \Rightarrow \quad \lambda_L > 16M_G B\lambda_x$$

so, in round numbers, and remembering this is just 1-D theory;  taking $M_G$~120, B~8, then

$$\boxed{\lambda_L[\mu m] \gtrsim \lambda_x[\mathring{A}]}$$

this is one motivating factor in the development of 2 um lasers



Zholents PRL 8 040701 (2005)

# ESASE

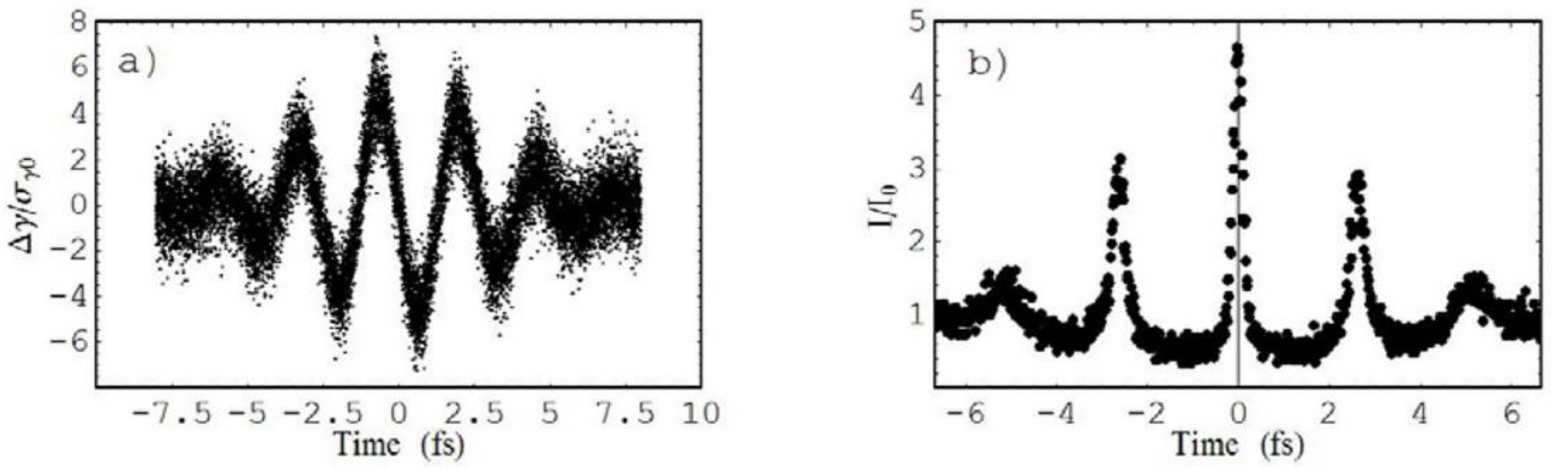


FIG. 5. Energy and peak current modulations produced in interaction with a few-cycle laser pulse. Only a part of the electron bunch affected by the interaction is shown.

Using a few-cycle Carrier Envelope Phase (CEP) stabilized IR pulse, a single attosecond pulse could be generated

- Lock CEP to 0
- Gain length of central current peak substantially shorter than satellite peaks



Zholents PRL 8 040701 (2005)

# ESASE: Start-to-end Simulations for LCLS

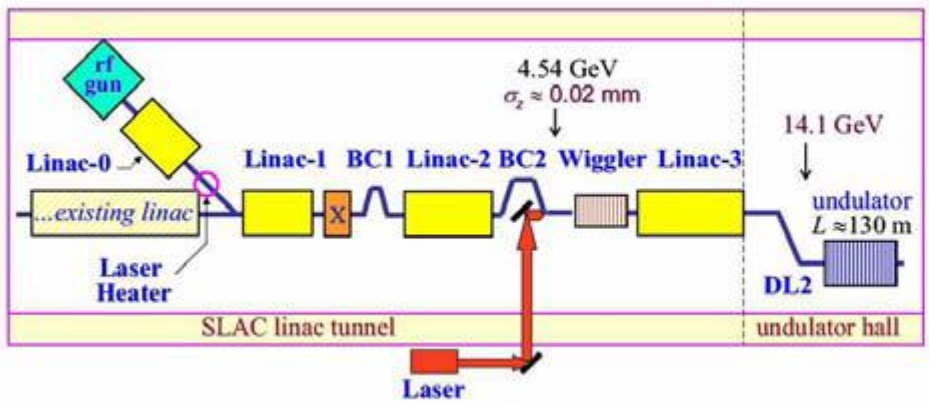


- modulation done at E=4.54 GeV
- existing dogleg functions as the chicane

Table 1: Energy modulator (EM) at 4.54 GeV for $B$=5 and two laser wavelengths ($\lambda_L$ =0.8 $\mu$m and 2.2 $\mu$m).

| Parameter | sym | 0.8 $\mu$m | 2.2 $\mu$m | unit |
|---|---|---|---|---|
| $N$ wiggler periods | $N_w$ | 8 | 8 | — |
| period of wiggler | $\lambda_w$ | 25 | 30 | cm |
| peak laser power | $P_{pk}$ | 9.7 | 10.7 | GW |
| laser rms waist | $\sigma_r$ | 0.25 | 0.25 | mm |
| modulation amp. | $\Delta\gamma$ | $\pm14$ | $\pm14$ | — |
| buncher $R_{56}$ | $R_{56}$ | 0.30 | 0.78 | mm |

- start-to-end simulation using PARMELA, ELEGANT, GINGER, and GENESIS
- $\lambda_L$ 0.8 $\mu$m and 2.2 $\mu$m, $\lambda_x$=0.15 nm
- 2 different focusing lattices
- CSR problems observed but likely to disappear in full 3-d simulation with finer resolution
- wakefields not fully included but are arguably small or manageable

Zholents et al SLAC-PUB-10713 (2004)

# ESASE: Start-to-end Simulations for LCLS

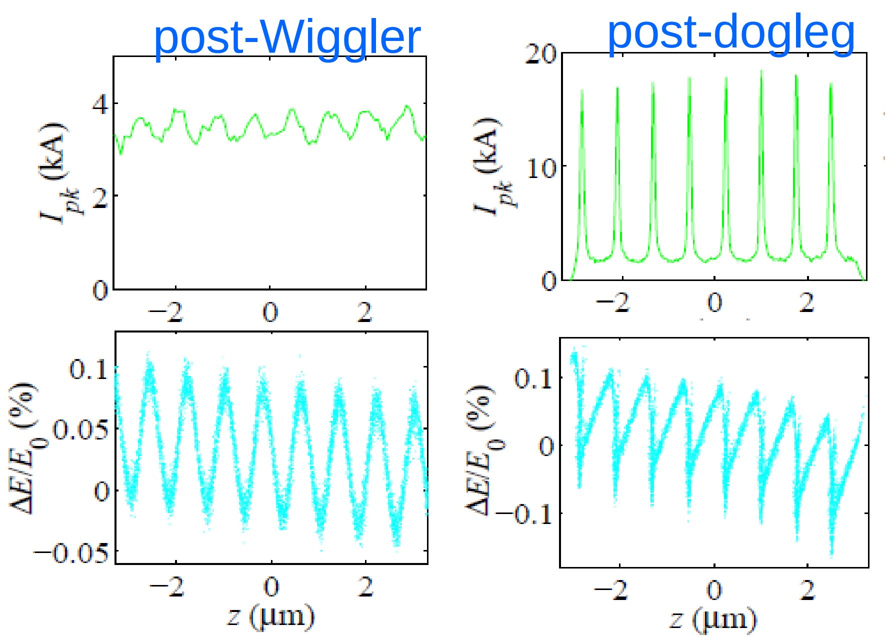


Table 2: Simulation results from GINGER and GENESIS.

| Param. | $\langle\beta\rangle = 26$ m | | | $\langle\beta\rangle = 12$ m | | unit |
|---|---|---|---|---|---|---|
| $\lambda_L$ | STD | 0.8 | 2.2 | 0.8 | 2.2 | $\mu$m |
| $L_{sat}$ | 70 | 58 | 57 | 44 | 45 | m |
| $\langle P\rangle$ | 13 | 2.0 | 3.0 | 2.9 | 7.6 | GW |
| $P_{spike}$ | 240 | 17 | 65 | 40 | 160 | GW |
| $\omega/\Delta\omega$ | 1500 | 550 | 660 | 660 | 790 | – |

- with 2.2 um, could reduce Lg<50 m
- SASE between peaks down $10^{-3}$

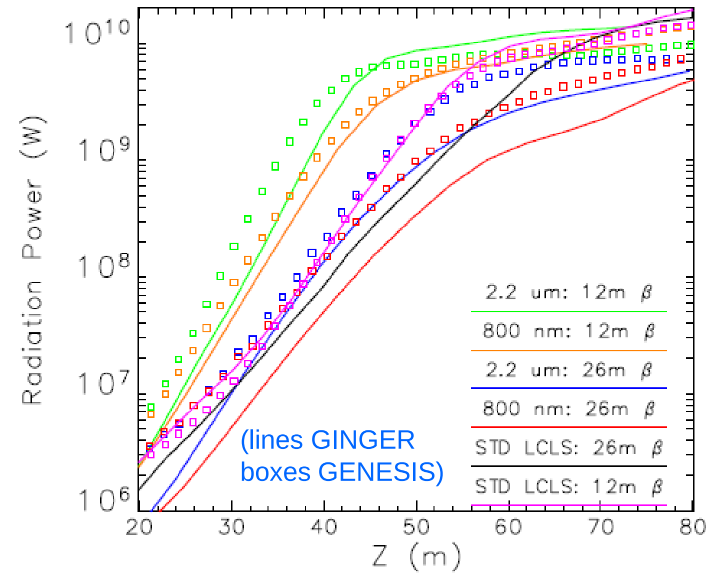


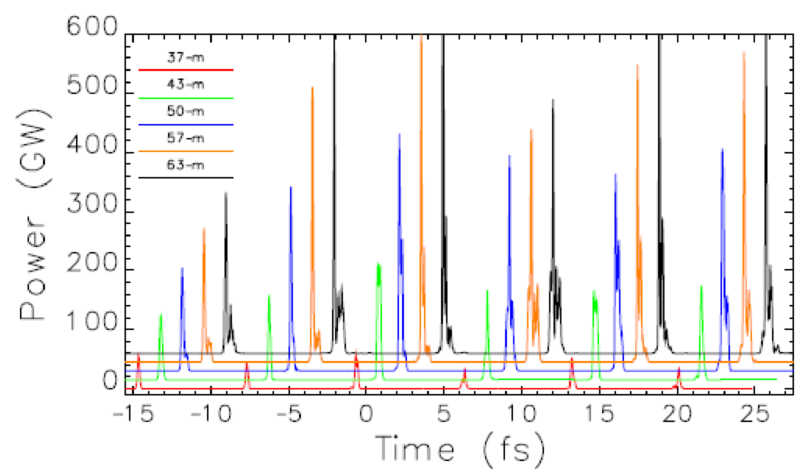


Figure 5: $P(t)$ snapshots at 5 different $z$-locations for a 2.2 $\mu$m-energy-modulated ESASE pulse with $\langle\beta\rangle$ =12 m, plotted with staggered offsets of 1.5 fs in time and 15 GW in power. For legibility, the $z$ =37 m data has been multiplied by a factor of 2.0.





Zholents et al SLAC-PUB-10713 (2004)

# Echo-enabled Harmonic Generation (EEHG)

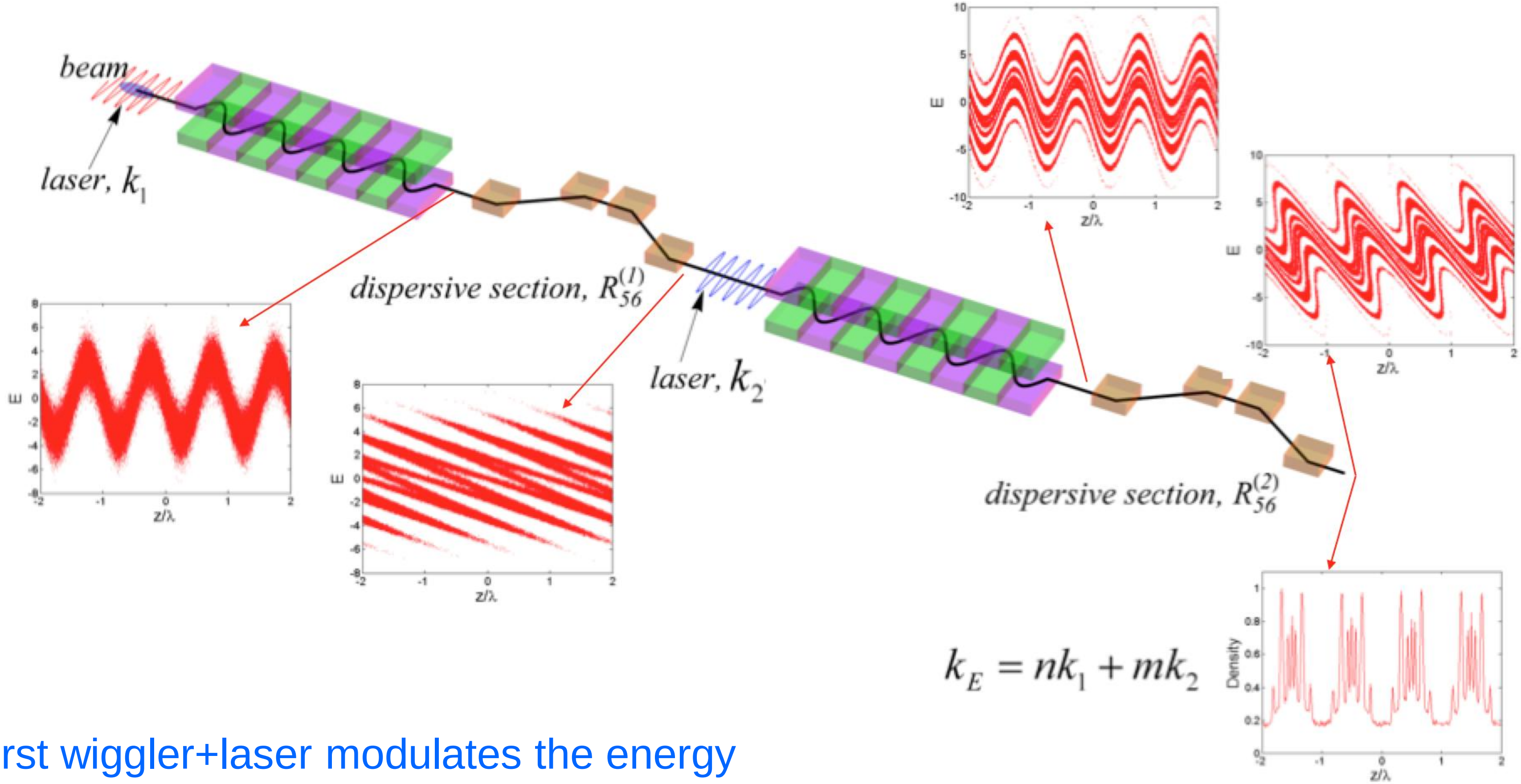


- First wiggler+laser modulates the energy
- First chicane creates energy bands of narrow width ($<<\sigma_{E0}$) at each z
- Second wiggler+laser modulates all of the bands
- Second chicane converts these modulations into density modulations at harmonics of the laser



https://portal.slac.stanford.edu/sites/ard_public/tfd/facilities/nlcta/Pages/Echo-enabled-Harmonic-Generation.aspx

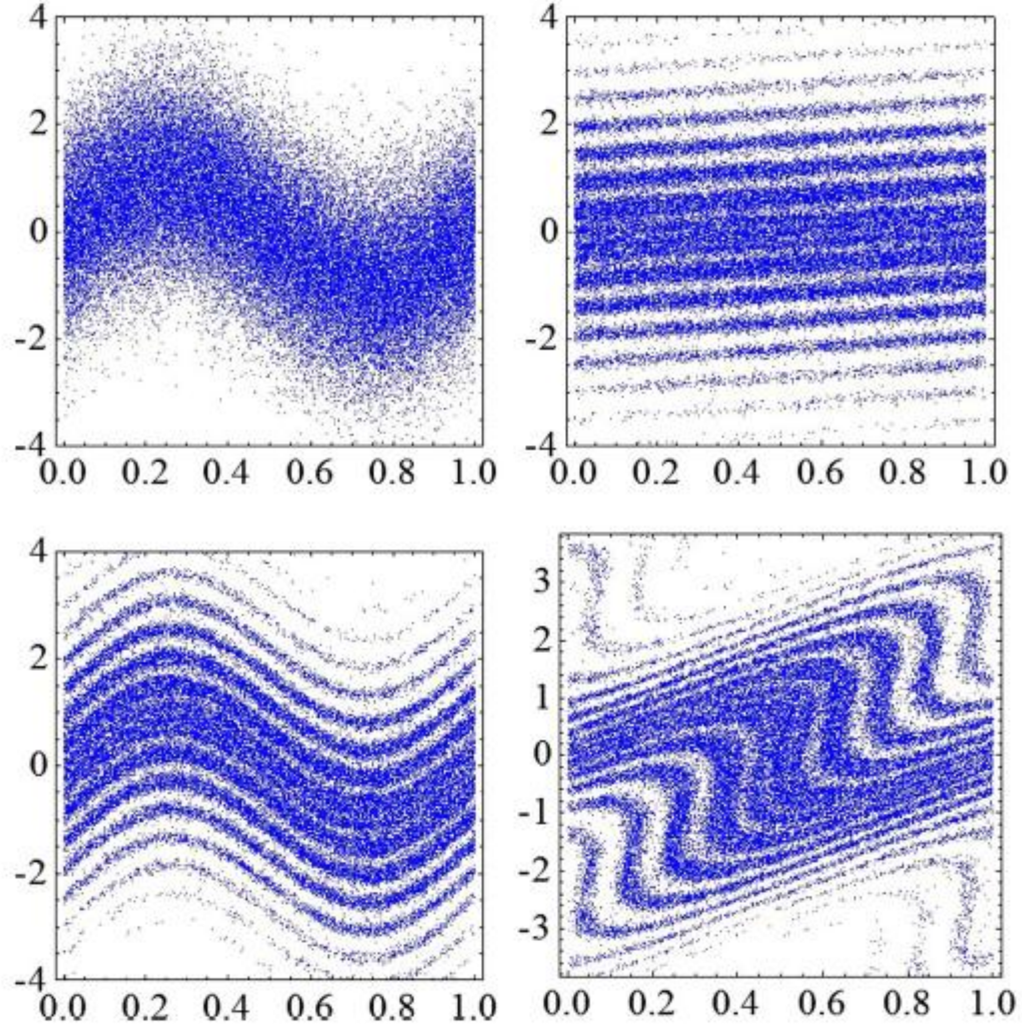


FIG. 3 (color online). The phase space of the beam after the first undulator (top left), the first dispersive element (top right), the second undulator (bottom left), and the second dispersive element (bottom right). Horizontal axes in the plots are $\zeta$, and the vertical axes are $p$.

G. Stupakov PRL 102, 074801 (2009)

# EEHG

- **Promises**
  - Remarkable up-frequency conversion efficiency: $b_n \sim n^{-1/3}$
  - Bunching AND Gain
  - UV laser -> soft x-rays in a single stage possible
  - Wide interest: China / France / Italy / Switzerland / UK / USA
- **Challenges**
  - Preservation of long-term (~ns) memory of phase space correlations
  - CSR/ISR in chicanes
  - Quantum diffusion in undulators
  - Unwanted $x$-$z$ coupling
  - Path length difference for particles with different betatron amplitude

slide from Dao Xiang's PAC11 talk

# EEHG demo at Shanghai DUV-FEL

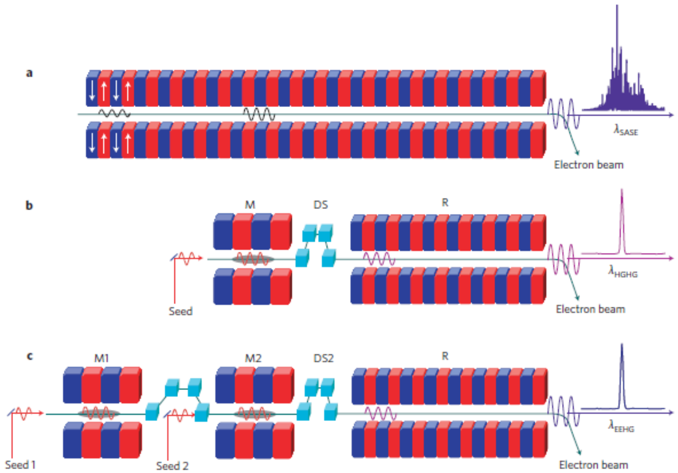


**Figure 1 | Seeded FEL versus SASE FEL.** **a**, SASE FEL, with poor temporal coherence. **b**, HGHG FEL, showing full temporal coherence with limited harmonic number ($N \approx 10$) for a single stage. **c**, EEHG FEL, showing full temporal coherence with a potentially very high harmonic number in a single stage. M, modulator; DS, dispersive section; R, radiator.

- 135 MeV beam energy limits experiment to 3rd harmonic of 1.05 um laser
- distinguish EEHG from HGHG by chirping the e-beam

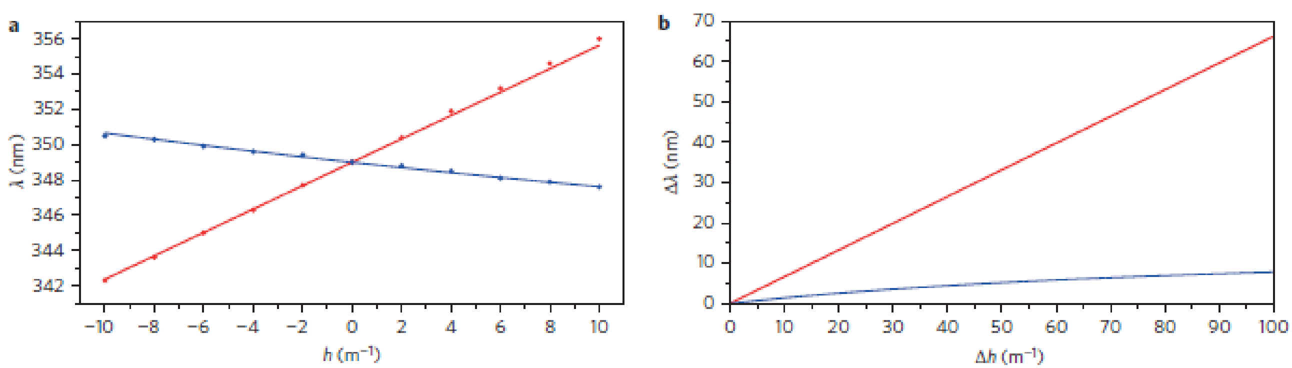


**Figure 2 | Spectral response to the energy chirp.** **a**, Central wavelength as a function of energy chirp of the electron beam (red filled circles, simulation results for HGHG; blue filled circles, simulation results for EEHG; red line, theoretical calculation for HGHG; blue line, theoretical calculation for EEHG). **b**, Spectral bandwidth as a function of total energy chirp in the electron beam (red line, theoretical calculation for HGHG; blue line, theoretical calculation for EEHG). $\Delta\lambda$, bandwidth of FEL radiation; $\Delta h$, total energy chirp in the electron beam.

Zhao et al Nat Phot 6, 360 (2012)

# EEHG demo at Shanghai DUV-FEL

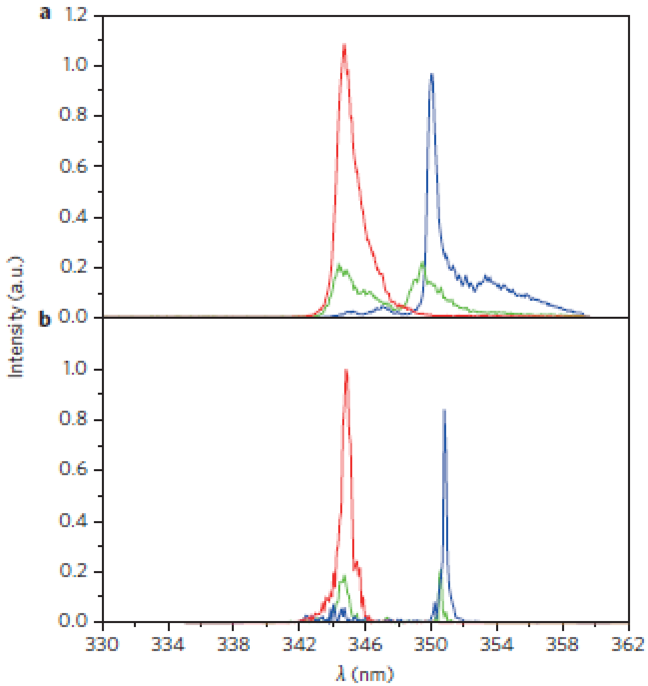


**Figure 3 | Spectra for FEL radiation. a**, Experimental results (red line, HGHG; blue line, EEHG; green line, intermediate state between HGHG and EEHG). **b**, Simulation results (red line, HGHG; blue line, EEHG; green line, intermediate state between HGHG and EEHG).

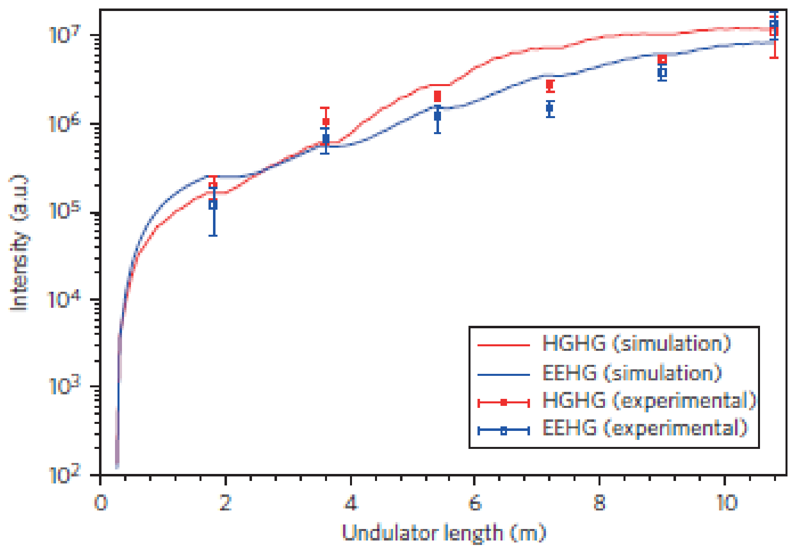


**Figure 5 | Gain curves of the EEHG and HGHG FEL at SDUV-FEL.** Intensity is measured with a calibrated CCD at the end of the radiator (red open squares, HGHG; blue open squares, EEHG). Error bars correspond to the peak-to-peak intensity statistics of 100 measurements. Simulation results are shown as a red line (HGHG) and a blue line (EEHG).

- Clear signature of EEHG
- Evidence also seen at SLAC's Next Linear Collider Test Accelerator at higher harmonic orders.

Zhao et al Nat Phot 6, 360 (2012)